



**Investigation of aged,  
size-resolved Asian  
dust storm particles**

H. Geng et al.

# Investigation of aged aerosols in size-resolved Asian dust storm particles transported from Beijing, China to Incheon, Korea using low-Z particle EPMA

H. Geng<sup>1</sup>, H. J. Hwang<sup>2</sup>, X. Liu<sup>3</sup>, S. Dong<sup>4</sup>, and C.-U. Ro<sup>5</sup>

<sup>1</sup>Institute of Environmental Science, Shanxi University, Taiyuan, 030006, China

<sup>2</sup>Korea Polar Research Institute, Songdo Dong, Yeonsu Gu, 406-840 Incheon, Korea

<sup>3</sup>Chinese Research Academy of Environmental Sciences, Anwai, Beiyuan, Dayangfang 8, Beijing 100012, China

<sup>4</sup>National Research Center for Environmental Analysis and Measurements, No.1 Yuhuanlu, Chaoyang District, Beijing 100029, China

<sup>5</sup>Department of Chemistry, Inha University, 253 Yonghyun-dong, Nam-gu, 402-751, Incheon, Korea

Received: 11 September 2013 – Accepted: 18 October 2013 – Published: 29 October 2013

Correspondence to: C.-U. Ro (curo@inha.ac.kr)

Published by Copernicus Publications on behalf of the European Geosciences Union.

Title Page

Abstract

Introduction

Conclusions

References

Tables

Figures



Back

Close

Full Screen / Esc

Printer-friendly Version

Interactive Discussion



## Abstract

This is the first study of Asian dust storm (ADS) particles collected in Beijing, China and Incheon, Korea during the same spring ADS event. Using a seven-stage May impactor and a quantitative electron probe X-ray microanalysis (ED-EPMA, also known as low-Z particle EPMA), we examined the composition and morphology of 4200 aerosol particles at stages 1–6 (with a size cut-off of 16, 8, 4, 2, 1, and 0.5  $\mu\text{m}$  in equivalent aerodynamic diameter, respectively) collected during an ADS event on 28–29 April 2005. The results showed that there were large differences in the chemical compositions between particles in sample S1 collected in Beijing immediately after the peak time of the ADS and in samples S2 and S3, which were collected in Incheon approximately 5 h and 24 h later, respectively. In sample S1, mineral dust particles accounted for more than 88 % in relative number abundance at stages 1–5, and organic carbon (OC) and reacted NaCl-containing particles accounted for 24 % and 32 %, respectively, at stage 6. On the other hand, in samples S2 and S3, in addition to approximately 60 % mineral dust, many sea salt particles reacted with airborne  $\text{SO}_2$  and  $\text{NO}_x$ , often mixed with mineral dust, were encountered at stages 1–5, and (C, N, O, S)-rich particles (likely a mixture of water-soluble organic carbon with  $(\text{NH}_4)_2\text{SO}_4$  and  $\text{NH}_4\text{NO}_3$ ) and K-containing particles were abundantly observed at stage 6. This suggests that the secondary aerosols and the internal mixture of mineral dust with sea spray aerosol increased when the ADS particles passed over the Yellow Sea. In the reacted or aged mineral dust and sea salt particles, nitrate-containing and both nitrate- and sulfate-containing species vastly outnumbered the sulfate-containing species, implying that ambient nitrogen oxides had a greater influence on the atmospheric particles during the ADS episode than  $\text{SO}_2$ . In addition to partially- or totally-reacted  $\text{CaCO}_3$ , reacted or aged Mg-containing aluminosilicates (likely including amesite, allophite, vermiculite, illite, and montmorillonite) were observed frequently in samples S2 and S3; and furthermore, both the atomic concentration ratios of  $[\text{Mg}]/[\text{Al}]$  and  $[\text{Mg}]/[\text{Si}]$  were elevated compared to that in sample S1. This shows that a great evolution or aging process must have occurred on the min-

## Investigation of aged, size-resolved Asian dust storm particles

H. Geng et al.

Title Page

Abstract

Introduction

Conclusions

References

Tables

Figures

◀

▶

◀

▶

Back

Close

Full Screen / Esc

Printer-friendly Version

Interactive Discussion



eral dust. This indicates that the number abundance, reactivity with gaseous pollutants, and ratios of  $[Mg]/[Al]$  and  $[Mg]/[Si]$  of Mg-containing aluminosilicates are promising indices of the aging process of ADS particles during long-range transport.

## 1 Introduction

Asian dust storms (ADSs), called “Ugalz”, “Huangsha”, “Whangsa”, and “Kosa” in Mongolia, China, Korea, and Japan, respectively, occur frequently in the arid and semiarid areas of Russia, Mongolia, and Northern China (Zhang et al., 2010; Natsagdorj et al., 2003). When Asian dust storm episodes occur, the desert dust can be blown eastward by strong winds over thousands of kilometers, being transported widely over East China, the Yellow Sea, the Korea Peninsula, Japan Island, and Pacific Ocean (Feng et al., 2002; Liu et al., 2013). Even the Arctic atmosphere is impacted by long-range transport of Asian dust (Iziomon et al., 2006). In the process of long-range transport, Asian dust is often mixed/reacted with various organic and inorganic materials (including gases, liquids, and aerosols), making their compositions extremely complicated (Song et al., 2013; Tobo et al., 2010).

The ACE-Asia (Aerosol Characterization Experiments-Asia) and other projects have found that there are substantial modifications in the chemical and physical properties of Asian dust during long-range transport based on detailed measurements of dust aerosols at ground-based, ship, aircraft, and satellite through “bulk” and individual particle analyses (Huebert et al., 2003; Zhang et al., 2006). Sea spray aerosols (SSAs) mixed internally and externally with mineral dust and the unique reactivity of calcium carbonate particles in the atmosphere when Asian dust passes over the sea have been reported (Krueger et al., 2003; Hwang and Ro, 2006; Zhang et al., 2006; Ma, 2010; Song et al., 2013). Calcium carbonate can neutralize sulfuric and nitric acids (generated by the oxidation of  $SO_2$  and  $NO_x$ , respectively) to form hygroscopic sulfates and nitrates (Usher et al., 2003), which often exhibit core-shell structures in “aged” particles (Yuan et al., 2006; Li and Shao, 2009). The formation of sulfate and nitrate coatings or

## Investigation of aged, size-resolved Asian dust storm particles

H. Geng et al.

Title Page

Abstract

Introduction

Conclusions

References

Tables

Figures

◀

▶

◀

▶

Back

Close

Full Screen / Esc

Printer-friendly Version

Interactive Discussion



**Investigation of aged,  
size-resolved Asian  
dust storm particles**

H. Geng et al.

Title Page

Abstract

Introduction

Conclusions

References

Tables

Figures

◀

▶

◀

▶

Back

Close

Full Screen / Esc

Printer-friendly Version

Interactive Discussion



secondary organic matter on minerals, sometimes mixed with SSAs, makes a significant contribution to the optical, chemical, and hygroscopic modification of Asian dust (Bauer et al., 2007; Kojima et al., 2004; Sullivan et al., 2007). This means that Asian dust acts as a significant carrier of pollutants to the downwind locations (Hatch and Grassian, 2008; Choi et al., 2001; Mori et al., 2003; Matsumoto et al., 2006) and the carrying ability is dependent to a large extent on the size, shape, and chemical components of the dust aerosols (Ma et al., 2004; Nie, et al., 2012; Wang, et al., 2013).

For the characterization of the complex mixtures of atmospherically-processed Asian dust aerosols in detail, many analytical techniques were utilized, in which the quantitative energy-dispersive electron probe X-ray microanalysis (ED-EPMA, also called low-Z particle EPMA) has proven to be a powerful and useful tool with a relatively short sampling time and without a complicated sample pretreatment process (Hwang and Ro, 2005, 2006; Geng et al., 2009a, 2011a, b). This single-particle analytical technique, which is based on scanning electron microscopy (SEM) coupled with an ultra-thin window energy-dispersive X-ray spectrometry (EDX), can simultaneously detect the morphology and constituent elements of individual particle and provide information on the aging process and transformation of many environmentally-important particles, such as nitrates, sulfates, and carbonaceous species (Maskey et al., 2010; Choël et al., 2005, 2007). For instance, through the application of low-Z particle EPMA to the characterization of airborne particle samples collected in the marine boundary layer (MBL) of the Bohai Sea and Yellow Sea on 30 April–1 May 2006, Geng et al. (2009a) suggested that Asian dust aerosols are important carriers of gaseous inorganic nitrogen species, especially  $\text{NO}_x$  and  $\text{NH}_3$ . The results obtained by low-Z particle EPMA showed an obvious contrast in chemical compositions between the atmospheric aerosol over King George Island, Antarctic and Ny-Ålesund, Svalbard, Arctic (Geng et al., 2010; Maskey, et al., 2011). Recently, the combined use of low-Z particle EPMA with attenuated total reflection Fourier transform infrared imaging technique (ATR-FTIR) and Raman microspectrometry (RMS) demonstrated that many individual Asian dust particles were

extensively chemically-modified (aged) and highly complicated in compositions (Song et al., 2013, 2010; Sobanska et al., 2012).

In the present study, low-*Z* particle EPMA was used to examine how size-resolved Asian dust contributes to ambient particulate matter in Beijing, China and Incheon, Korea in a same ADS event occurred in April 2005 and to examine the heterogeneous aging of Asian dust particles when they transported from China to Korea over the Yellow Sea. This study presents the detailed characterization of reacted or aged mineral dust and SSAs, which became physically and chemically altered during long-range transport through interactions with anthropogenic gaseous pollutants and marine aerosols. Special emphasis has been placed on quantitative analysis of the elemental percentages of different stages, samples, and types for reacted particles in the size range of 0.2–10 μm. The changes in the ratios of [Na]/[Cl], [N]/[Cl], and [S]/[Cl] in the aged SSAs and the changes of [Mg]/[Al] and [Mg]/[Si] in the aged aluminosilicates will be investigated. To the best of the authors' knowledge, this is the first report of the results for ADS particles collected in Beijing and Incheon during the same spring ADS episode. The investigation of the chemical compositions of size-resolved Asian dust storm particles collected in the two sites and identification of reacted or aged aerosols would help improve the understanding of the sources, reactivity, transport, and removal of mineral dust particles, as well as the heterogeneous reaction processes between air pollutants and mineral dust.

## 2 Materials and methods

### 2.1 Sampling sites and dates

The two sampling sites were located in Beijing, China and Incheon, Korea (Fig. 1). In Beijing, immediately after the peak of an ADS event on 28 April 2005, aerosols were collected on the roof of a building in the Chinese Research Academy of Environmental Sciences (39°59' N, 116°25' E), approximately 30 m.a.g.l. (notated as sample S1 here-

ACPD

13, 27971–28016, 2013

## Investigation of aged, size-resolved Asian dust storm particles

H. Geng et al.

Title Page

Abstract

Introduction

Conclusions

References

Tables

Figures

◀

▶

◀

▶

Back

Close

Full Screen / Esc

Printer-friendly Version

Interactive Discussion



after; Table 1). Approximately 5 and 24 h later, samplings were conducted on the roof of a five-story building in Inha University (latitude 37.45° N, longitude 126.73° E, approximately 25 m a.g.l.) in Incheon. The first sampling in Incheon was carried out at 15:00 ~ 18:55 (KST) on 28 April 2005 when the ADS event began (sample S2) and the second was at the peak time of the ADS event on 29 April 2005 (sample S3). Figure 2 shows the hourly PM<sub>10</sub> values recorded in Beijing and Incheon during four consecutive days from 27 to 30 April 2005. In Beijing, the 24 h average PM<sub>10</sub> concentrations reached 706 µg m<sup>-3</sup> on 28 April 2005, which is approximately five times higher than the Chinese state Grade-II standard of 150 µg m<sup>-3</sup> and hourly PM<sub>10</sub> exceeded 1500 µg m<sup>-3</sup> for five consecutive hours with the peak level of 3198 µg m<sup>-3</sup> (at approximately 7 o'clock on 28 April 2005, KST). The PM<sub>10</sub> concentrations in Incheon, which were recorded at an air quality monitoring station (Sungui-dong, Nam-gu), close to the sampling site, exceeded the Korean National Ambient Air Quality Standard (100 µg m<sup>-3</sup> on the daily average) with 158.2 µg m<sup>-3</sup> on 29 April 2005. The hourly PM<sub>10</sub> levels exceeded 100 µg m<sup>-3</sup> for 28 consecutive hours and reached up to 308 µg m<sup>-3</sup> at the peak time of the ADS episode. The PM<sub>10</sub> level in Incheon was ten times lower than the maximum value recorded in Beijing due to the dispersion and removal of ADS particles during long-range transport.

The particles were collected on Ag and Al foils using the seven-stage May cascade impactor. At a flow rate of 20 L min<sup>-1</sup>, the May impactor has nominal aerodynamic cut-off diameters of 16, 8, 4, 2, 1, 0.5, and 0.25 µm for stages 1–7, respectively. The number-size distribution of ambient particles was monitored in situ using an optical particle counter to observe the particle number concentration. To prevent the overloading of particles at the impaction slots, the sampling durations were adjusted according to the atmospheric particle load, varying between 30 s (for particles on stage 6) and 2 h (for particles on stage 1). The collected samples were placed in Petri dishes, sealed, and stored in a desiccator prior to the measurements.

# Investigation of aged, size-resolved Asian dust storm particles

H. Geng et al.

Title Page

Abstract

Introduction

Conclusions

References

Tables

Figures

◀

▶

◀

▶

Back

Close

Full Screen / Esc

Printer-friendly Version

Interactive Discussion



## 2.2 Measurement and analysis

The size, morphology, and chemical composition of the individual aerosol particles were determined by a scanning electron microscopy (SEM) equipped with an Oxford Link SATW ultrathin window energy-dispersive X-ray spectrometry detector (Hitachi S-3500N). The resolution of the detector was 133 eV for Mn-K $\alpha$  X-rays. The X-ray spectra were recorded under the control of INCA software. An accelerating voltage and beam current of 10 kV and 1.0 nA, respectively, were chosen to achieve the optimal experimental conditions, such as low background level and high sensitivity for low-Z element analysis. A typical measuring time of 10 s was used to limit the beam damage on sensitive particles. The secondary electron images (SEIs) and X-ray spectra of 100 particles on stages 1 and 6 and 300 particles on stages 2 to 5, respectively, were detected (1400 particles per sample). In total, 4200 particles were analyzed for the three samples. The particle equivalent diameters were estimated from their projected area, assuming the particles to be spherical. The methods for acquiring the net X-ray intensities of the elements, for simulating the measured X-ray intensities for all chemical elements in a particle by Monte Carlo calculations, and using the “expert system” program to perform chemical speciation and determine the particle group distributions are described elsewhere (Vekemans et al., 1994; Ro et al., 2003, 2004). The elemental quantification procedure provided results with an accuracy of within 12 % relative deviations between the calculated and nominal elemental concentrations for various standard particles (Ro et al., 2000, 2001).

## 2.3 Backward trajectories for the air mass transport history

The 48 h backward air-mass trajectories at receptor heights of 500 m, 1000 m, and 2000 m.a.s.l. were produced using the HYbrid Single-Particle Lagrangian Integrated Trajectory (HYSPLIT4) model available at the NOAA Air Resources Laboratory’s web server (<http://www.arl.noaa.gov/ready/hysplit4.html>). As shown in Figs. 1 and 3, the dust cloud, which originated from Mongolia (likely from the Gobi Desert), moved over

ACPD

13, 27971–28016, 2013

### Investigation of aged, size-resolved Asian dust storm particles

H. Geng et al.

Title Page

Abstract

Introduction

Conclusions

References

Tables

Figures

◀

▶

◀

▶

Back

Close

Full Screen / Esc

Printer-friendly Version

Interactive Discussion





Inner Mongolia and Beijing city and was dispersed southeast toward the Korean peninsula.

### 3 Results and discussion

#### 3.1 Particle size on different collecting stages

5 The particle size is closely related to the chemical compositions, heterogeneous reactivity, and ultimate fate of ambient particles (Formenti et al., 2011). The mean equivalent diameters of all 4200 particles analyzed in the stages 1–6 are  $15.6 \pm 7.0$ ,  $7.5 \pm 2.6$ ,  $3.8 \pm 1.4$ ,  $2.3 \pm 1.0$ ,  $1.3 \pm 0.6$ ,  $0.9 \pm 0.6 \mu\text{m}$  in size, respectively (Table 2), which has minor deviation compared to the nominal aerodynamic cut-off diameters of the May impactor (with 50 % efficiency of 16, 8, 4, 2, 1, and  $0.5 \mu\text{m}$  for stages 1–6, respectively). Possibly, some size misclassification might have occurred due to particle bounce-off during sampling (Hwang et al., 2008). The particles on stage 6 in sample S1 were significantly smaller than those in both samples S2 and S3 because many hygroscopic particles which look dark and “big” in size on their secondary electron images (SEIs) were encountered on stage 6 of samples S2 and S3 (Figs. 4 and 5). Also, as seen in Fig. 6, a lot of hygroscopic particles were encountered on stage 4 of samples S2 and S3 (Fig. 6).

The particle size will change during mixing or reactions between the different types of particles. As illustrated in Fig. 4, the particles on stage 1 had a similar distribution trend in samples S1–S3, but for the particles on stages 2 and 3, those in sample S1 tended to be larger than those in samples S2 and S3 because they have lower percentage in the smaller size range ( $\sim 21\%$  in the size range of  $4\text{--}6 \mu\text{m}$  in diameter for stage 2 and  $2\text{--}3 \mu\text{m}$  for stage 3 compared to more than  $40\%$  in those size ranges in samples S2 and S3). The trend was opposite for the particles in stages 4 and 6. The particles on stages 4 and 6 in sample S1 have a higher percentage in the smaller size range than those in samples S2 and S3 ( $\sim 70\%$  vs.  $40\%$  in the  $1\text{--}2 \mu\text{m}$  size



range for stage 4 and 90 % vs. 60 % in 0.1–1  $\mu\text{m}$  size range for stage 6). This suggests that the smaller particles collected in Incheon tend to become larger, due likely to mixing between particles (e.g., dust particles mixed with sea salt) or reactions between particles and gas/liquid substances (e.g., dust particles reacted with  $\text{NO}_x$  and  $\text{SO}_2$ ).

5 Indeed, the chemical compositions of the particles differed according to the size range, as shown in Figs. 7 and 8.

### 3.2 Classification of measured particles

The way to determine the chemical species of individual particles and perform a classification based on their chemical species is summarized briefly. Firstly, the particles were regarded to be composed of just one chemical species when the chemical species constituted at least 90 % of the atomic fraction. Secondly, efforts were made to determine the chemical species of the internally mixed particles based on all the chemical species identified. Thirdly, elements with less than 1 at.% were neglected in the chemical speciation because the elements at trace levels cannot be investigated reliably. Although the presence of hydrogen cannot be detected in EPMA, elemental carbon (EC) and organic carbon (OC) could be identified based on their morphologies and the contents of C and O (Geng et al., 2011a). The particles were grouped into different types according to the criteria summarized in Table 3. Overall, ten groups of particles were classified. They are unreacted mineral dust; aged or reacted mineral dust; fresh SSA (or NaCl-containing); reacted (or aged) SSA (and mixtures) or reacted NaCl-containing; EC; OC; (C, N, O, S)-rich particle; K-containing particles; Fe-rich particles; and others. Figures 5 and 6 show SEIs of various types of particles.

Title Page

Abstract

Introduction

Conclusions

References

Tables

Figures

◀

▶

◀

▶

Back

Close

Full Screen / Esc

Printer-friendly Version

Interactive Discussion



### 3.3 Chemical compositions of size-resolved particles in samples S1, S2, and S3

#### 3.3.1 Particles on stages 1–5

3900 particles on stages 1–5 of samples S1–S3 (1300 for each sample) were analyzed. Based on the classification of the particles, the relative number abundances of the various particle types were obtained by dividing the number of a specific type of particles by the total number of particles analyzed for each stage, as shown in Fig. 7. By comparing the relative abundances of the major particle types at different size levels, there were significant differences in the aerosol components between the three samples, reflecting the aging process of the ADS particles. Detailed description on the change in the relative abundances of various types of particles is summarized as follows.

#### Mineral dust particles

Mineral dust particles appear irregular and bright on their SEIs. The typical unreacted mineral dust particles include aluminosilicate,  $\text{SiO}_2$ ,  $\text{CaCO}_3$ ,  $\text{CaMg}(\text{CO}_3)_2$ , and  $\text{TiO}_2$  (Shao et al., 2008). The reacted (or aged) mineral dust particles mainly include “reacted  $\text{CaCO}_3/\text{CaMg}(\text{CO}_3)_2$ ” and “aluminosilicate + (N, S)”, where the (N, S) notation represents compounds containing either nitrates, sulfates, or both. They were either produced when mineral dust particles (particularly  $\text{Ca}^{2+}$ -containing species) react with airborne sulfur and nitrogen oxides in the presence of moisture or with “secondary acids”, such as  $\text{H}_2\text{SO}_4$ ,  $\text{HNO}_3$ , and  $\text{HCl}$  (Harris et al., 2012; Wang et al., 2005), or were formed from the adsorption of  $\text{NH}_4\text{NO}_3$  or  $(\text{NH}_4)_2\text{SO}_4/\text{NH}_4\text{HSO}_4$  on the particle surface (Sullivan et al., 2007). In the present study, the overall relative abundance of mineral dust particles (i.e. aluminosilicate, calcite, dolomite, quartz, etc.) was more than 88 % of the particles analyzed for sample S1 collected in Beijing. On the other hand, for samples S2 and S3 collected in Incheon, the relative abundances of mineral dust

Investigation of aged,  
size-resolved Asian  
dust storm particles

H. Geng et al.

Title Page

Abstract

Introduction

Conclusions

References

Tables

Figures

◀

▶

◀

▶

Back

Close

Full Screen / Esc

Printer-friendly Version

Interactive Discussion



particles were smaller than that of sample S1. The mixture of reacted SSA with mineral dust that were not encountered in sample S1 were frequently observed in samples S2 and S3. Overall, the reacted (aged) mineral dust particles have higher abundance than the unreacted ones on stages 1–5: approximately 71 % vs. 17 % (~ 4.2 fold) on average for sample S1; 50 % vs. 6 % for sample S2; and 48 % vs. 13 % for sample S3 (Fig. 7). And the majority of aged mineral dust particles are nitrate-containing species and both sulfate- and nitrate-containing species (Tables 4 and 5). This is consistent with the results for aerosol particles collected in the marine-atmospheric boundary layer of the Yellow Sea when an Asian dust storm passed by (Geng et al., 2009a). The relative abundances of reacted  $\text{CaCO}_3$  or  $\text{CaMg}(\text{CO}_3)_2$  in sample S1 is generally lower than that in samples S2 and S3, whereas the unreacted samples showed an opposite trend, suggesting that some atmospheric reactions might have occurred on the surface of the particles when they passed over the Yellow Sea (Fairlie et al., 2010; Ma et al., 2004; Wang et al., 2005). In sample S1, the relative abundance of the reacted  $\text{CaCO}_3$  or  $\text{CaMg}(\text{CO}_3)_2$  was 3 % (in which the nitrate-containing species account for 97 %), which is similar to that of the unreacted samples. On the other hand, in samples S2 and S3, the reacted  $\text{CaCO}_3$  or  $\text{CaMg}(\text{CO}_3)_2$  largely outnumbered the unreacted ones (13 % vs. 1 % in sample S2 and 11 % vs. 2 % in sample S3, respectively), indicating that moisture over the sea might play important roles in enhancing the reactions of  $\text{CaCO}_3$  or  $\text{CaMg}(\text{CO}_3)_2$  with  $\text{NO}_x$  or  $\text{SO}_2$  (Formenti et al., 2011).

The aluminosilicate particles with strong X-ray peaks of Al, Si, and O and minor elements, such as Na, K, Ca, Fe, Cl, Ti, etc., are important components of mineral dust. They exist in many different forms, including Na-feldspar, K-feldspar, muscovite, montmorillonite, illite, Mg-vermiculite, kaolinite, talc, pyrophyllite, etc. (Jung et al., 2010; Malek et al., 2011). Most of them belong to clay mineral. Table 5 lists the elemental compositions of different types of aluminosilicates and their respective relative abundances. The reacted or aged aluminosilicates greatly outnumbered the unreacted ones in all samples (on average, 58 % vs. 12 % in sample S1, 4.8 fold; 33 % vs. 3 % in sample S2, 11 fold; and 35 % vs. 8 % in sample S3, 4.4 fold). This has a similar distribution

Investigation of aged,  
size-resolved Asian  
dust storm particles

H. Geng et al.

Title Page

Abstract

Introduction

Conclusions

References

Tables

Figures

◀

▶

◀

▶

Back

Close

Full Screen / Esc

Printer-friendly Version

Interactive Discussion



trend to the reacted  $\text{CaCO}_3$  in the three samples, i.e. more aged mineral dusts were produced in sample S2, possibly being related to their transport path. Moreover, most reacted or aged aluminosilicates contain nitrates. Those containing only sulfates without nitrates are rarely encountered, indicating that aluminosilicate particles react more easily with  $\text{NO}_2$  or  $\text{HNO}_3$  than with  $\text{SO}_2$  or  $\text{H}_2\text{SO}_4$ .  $\text{NH}_4\text{NO}_3$  adsorbed on the surface of aluminosilicate particles cannot be excluded.

In aluminosilicates, many of them contain magnesium (Mg). The Mg-containing species in unreacted aluminosilicates account for 73 %, 46 %, and 40 % in samples S1–S3, respectively, on average; and in the reacted or aged aluminosilicates, they account for 74 %, 63 % and 63 % in samples S1–S3, respectively. Corresponding to the mineralogy, the particles with X-ray peaks of Al, Si, O, and Mg in the EDX spectra are considered amesite or allophite, normally associated with chlorite, magnetite, rutile, diasporite, calcite, grossular, diopside, and clinozoisite in a range of locations. The particle showing strong X-ray peaks for Al, Si, O, Mg, and Fe might be a Mg-vermiculite, likely being formed by weathering or hydrothermal alterations of iron-bearing phlogopite and annite (Malek et al., 2011). In addition, Mg signals also can be observed in illite and montmorillonite. They were commonly observed in airborne particles collected during ADS events (Xuan et al., 2004; Schulz et al., 2012; Sobanska et al., 2012). These Mg-containing aluminosilicates are abundant in the soils of Chinese loess areas and desert areas (Malek et al., 2011; Takahashi et al., 2010). Therefore, it is expected that they would be uplifted in the air and transported to the area when an ADS occurs. Herein, they were simplified as the groups of (Al, Si, O, Mg) and (Al, Si, O, Mg) and mixtures, in which the mixture includes one or more of Na, Fe, Ca, K, Cl, P, and Ti (Table 5). The relative abundance of Mg-containing aluminosilicates ( $\text{AlSiOMg}$  and  $\text{AlSiOMg}/(\text{mixture})$  species) in Beijing is larger than that in Incheon (on average, 74 % in sample S1 vs. 55 % and 51 % in samples S2 and S3). Moreover, the calculated atomic concentration ratios show an obvious increase in  $[\text{Mg}]/[\text{Al}]$  and  $[\text{Mg}]/[\text{Si}]$  in samples S2 and S3 compared to sample S1, both for the unreacted and reacted (aged) aluminosilicate particles (Fig. 9). This suggests that some reactions in aluminosilicates

(particularly Mg-containing species) must have occurred so that their chemical compositions were changed. It implies that Mg-containing aluminosilicates play important roles in understanding the heterogeneous aging process of mineral dust when they pass over the Yellow Sea.

## 5 Sea spray aerosols (SSAs)

Figure 10 shows the relative abundance of fresh and reacted (aged) SSA at stages 1–5. As no SSA was encountered in sample S1, SSAs in samples S2 and S3 should have originated from the Yellow Sea. Moreover, the SSA's relative abundance in sample S2 outnumbers that in sample S3, particularly for stage 5. The fresh SSA particles, which were identified by the presence of Na and Cl peaks and often with minor C, O, Mg, and Ca signals in their X-ray spectra, were encountered only in sample S2 with low abundance: less than 1 % on stage 2, stage 4, and stage 5. On the other hand, many aged or reacted SSA particles were encountered in samples S2 and S3, suggesting that the aerosols were largely influenced by airborne  $\text{NO}_x$  and/or  $\text{SO}_2$ .

Low-Z particle EPMA can clearly distinguish between partially- and totally-reacted SSAs. The former are observed as nitrates and sulfates of sodium and magnesium with residual chlorine, whereas the later are found in the form of just Na and N and/or S with little Cl being detected in the X-ray spectra (Geng et al., 2009a, 2009b). In particular, this method provides the possibility of quantitative analysis of the elemental percentages in SSAs among different stages and samples. The changes in the Cl/Na ratio, Cl/N ratio, and S/Cl ratio can reflect the Cl depletion of reacted SSAs to some extent, as shown in Table 6. The reacted or aged SSAs were classified into three types based on their SEIs and X-ray spectral data. The first was for those containing nitrates, such as  $\text{Na}(\text{Cl}, \text{NO}_3)$  and  $(\text{Na}, \text{Mg})(\text{Cl}, \text{NO}_3)$ . The second was for those containing sulfates ( $\text{SO}_4^{2-}$ ) or methanesulfonate ( $\text{CH}_3\text{SO}_3^-$ ), which were generated from the reactions of sea salt with anthropogenic  $\text{SO}_2/\text{H}_2\text{SO}_4$  and/or methylsulfonic acid (MSA) from the oxidization of dimethylsulfide (DMS) (Hopkins et al., 2008; Yang et al., 2009). It can be

Title Page

Abstract

Introduction

Conclusions

References

Tables

Figures

◀

▶

◀

▶

Back

Close

Full Screen / Esc

Printer-friendly Version

Interactive Discussion



noted that sulfate popularly exists in sea salt. Ault et al. (2013) reported that nascent SSAs sampled immediately after formation through bubble bursting have sulfate without any time for reaction with oxidized DMS products. Although  $\text{SO}_4^{2-}$  and  $\text{CH}_3\text{SO}_3^-$  are likely to be present simultaneously in sulfur-containing aged SSAs, sulfate-containing aerosols generated from oxidized DMS can be neglected because the contribution of biologically produced DMS to sea-salt sulfate is not significant over the Yellow Sea and Bohai Sea compared to the anthropogenic contributions (Yang et al., 2009). The third was for those containing both  $\text{NO}_3^-$  and  $\text{SO}_4^{2-}/\text{CH}_3\text{SO}_3^-$ . In addition, the reacted SSAs mixed internally with mineral dust species (such as  $\text{CaCO}_3$  and aluminosilicates) were classified into the group of “reacted sea salt and mixture”. In this study, the range of S/Na ratio in all the reacted or aged SSAs is in 0.5–1.08 (Table 6), largely more than that in seawater: ca. 0.083 (Maskey et al., 2011). Compared to the non-sea-salt sulfate, sea-salt sulfate accounts for minor in the reacted SSAs. Those containing  $\text{NO}_3^-$  significantly outnumbered the  $\text{SO}_4^{2-}/\text{CH}_3\text{SO}_3^-$  and both-containing ones on stages 1–5 (Fig. 10). The mixtures of aged SSAs with mineral dust are encountered frequently on stages 2–5. They account for 65 % on average in sample S2 (58 %, 67 %, 68 %, and 67 % in stages 2–5, respectively) and 60 % in sample S3 (71 %, 61 %, 58 %, and 48 % in stages 2–5, respectively), suggesting that the internal mixing of sea salt and mineral dust occurred during the ADS event mainly after the particles left the continent. This indicates that ADS particles experienced chemical reactions during their long-range transport over the sea. At least many of them were mixed with SSAs by collision or coagulation or by in-cloud processes (Ma, 2010).

## Carbonaceous particles

EC (also termed as a “carbon-rich” particle) and OC particles are ubiquitous in the atmosphere and contribute significantly to the suspended particulate matter both in remote and urban locations (Sudheer et al., 2008; Arimoto et al., 2006). In this study, EC particles are in low abundances on stages 1–5 (~ 2 % on average for each sam-

## Investigation of aged, size-resolved Asian dust storm particles

H. Geng et al.

Title Page

Abstract

Introduction

Conclusions

References

Tables

Figures

◀

▶

◀

▶

Back

Close

Full Screen / Esc

Printer-friendly Version

Interactive Discussion



ple) compared to OC particles (7 %, 16 %, and 17 % on average for samples S1–S3, respectively) (Fig. 7), suggesting that OC particles are dominant in the carbonaceous aerosols for the ADS particles. Furthermore, the abundance of OC particles collected in Incheon (samples S2 and S3) outweighs that collected in Beijing (sample S1), suggesting that many OC particles come from the atmosphere over the Yellow Sea during the ADS event.

### (C, N, O, S)-rich particles

The (C, N, O, S)-rich particles were encountered at stage 5 in sample S3. EDX revealed peaks for C, O, S, and N and their SEIs showed round, dark shape. These particles are considered as  $(\text{NH}_4)_2\text{SO}_4/\text{NH}_4\text{HSO}_4$ -containing particles, a secondary species produced from the reactions of ambient sulfate or sulfuric acid with ammonia (largely emitted from regions of high agricultural activity and livestock farming) (Geng et al., 2009b).  $\text{NH}_4\text{NO}_3$ , which is formed by a reaction of ambient  $\text{NO}_2$  or  $\text{HNO}_3$ , might be included in this type of particle because the N concentration is much larger than the S concentration in some of this type of particles (Fig. 11). These will be described in detail in Sect. 3.3.2 because (C, N, O, S)-rich particles were observed abundantly in the stage 6 samples.

### Fe-rich and other particles

Fe-rich particles appear bright and irregular on their SEIs and normally contain strong Fe and O peaks in their X-ray spectra, sometimes with minor C, Si, and Al. Several of them are shown in Figs. 5 (particles #2, #5, and #41) and 6 (particle #52). These particles are in the form of iron ((oxy)hydr)oxides, and are interpreted as goethite, hematite, or magnetite in atmospheric aerosols. Human activities, such as mining, steel production, metallurgical industries, the abrasion of brake linings, and erosion of asphalted road, might lead to significantly higher loads of Fe/ $\text{FeO}_x$  (Flament et al., 2008). Sometimes, ADS carry various fractions of fine-grained magnetic particles, containing mainly

## Investigation of aged, size-resolved Asian dust storm particles

H. Geng et al.

Title Page

Abstract

Introduction

Conclusions

References

Tables

Figures

◀

▶

◀

▶

Back

Close

Full Screen / Esc

Printer-friendly Version

Interactive Discussion





$\text{Fe}_3\text{O}_4$  and  $\gamma\text{-Fe}_2\text{O}_3$  (Kim et al., 2012). On the other hand, in the present study, Fe-rich particles at stages 1–5 have average abundance of 2 %, 1 %, and 4 % in samples S1–S3, respectively. This means that the ADS did not increase the level of Fe-rich particles significantly in Incheon.

### 3.3.2 Particles on stage 6

The compositions of particles on stage 6 and stages 1–5 differed significantly. As shown in Fig. 8, many aged NaCl-containing particles ( $< 1\ \mu\text{m}$  in diameter) were encountered in sample S1 with an abundance of approximately 32 %. This is surprising. Their morphologies in SEI (particle #3 in Fig. 5a) and the information from the backward air-mass trajectory (Fig. 3a) show that they are different from the sea salt particles from the Yellow Sea. The highest possibility is that they might come from dried salt lakes near Hunshandake Sandy Land or Hulunbeier Sandy Land in the southeast and northeast, respectively, of the Inner Mongolia plateau (Zhang et al., 2010). Huang et al. (2010) and Sun et al. (2010) also reported that NaCl-containing particles were observed in Beijing when an ADS passed by.

Notably, there were many (C, N, O, S)-rich particles in samples S2 and S3 (Fig. 8), whereas none were observed in sample S1, suggesting that many secondary aerosols were generated when the ADS moved into Incheon. Although their formation mechanism is beyond this study, it appears that the  $(\text{NH}_4)_2\text{SO}_4/\text{NH}_4\text{NO}_3$ -containing particles mixed with water-soluble organic matter were formed favorably due to the elevated humidity in the air when the air masses carrying Asian dust as well as  $\text{SO}_2$ ,  $\text{NO}_2$ , and  $\text{NH}_3$  passed over the sea. Under high humidity, the uptake of water/moisture, water-soluble organic carbon, and gaseous pollutants will enhance the generation of (C, N, O, S)-rich particles.  $\text{NH}_4\text{NO}_3$  is likely to be included because  $\text{NH}_4\text{NO}_3$  is water-soluble and the measured N levels are sometimes much larger than S (Fig. 11). Herein, the (C, N, O, S)-rich particles have higher abundance on stage 6 in samples S2 and S3 and are barely encountered on the other stages (except on stage 5 in sample S3, with 8.3 % in abundance), suggesting that they are small in size and are generated in the

high-humidity atmospheric environment, likely becoming droplets in the air. In addition, there are higher abundances of OC-containing particles in sample S1 than samples S2 and S3 (23.6 % vs. 7.7 % and 9.6 %), showing that the OC particles on stage 6 are abundant in Beijing. Possibly, they were dissolved in water and absorbed into the (C, N, O, S)-containing droplet particles during transport when they passed over the sea.

K-containing particles, mostly from biomass burning (Wang et al., 2007; Andreae, 1983), are encountered only on stage 6. Furthermore, they have much less abundance in sample S1 than in samples S2 and S3 (2.4 % vs. 15.4 % and 15.4 %) (Fig. 8), suggesting that there are sources of biomass burning near Beijing or Incheon (Shen et al., 2007; Liu et al., 2000, 2005).

### 3.4 Mixing and aging processes of ADS particles during long-range transport

The air mass backward trajectory shows that this ADS originated mainly from the Gobi Desert in Mongolia, passing over arid and semi-arid regions of China (including the Inner Mongolia Autonomous Region and Hebei Province), and arriving at Beijing (Fig. 3). The particles then passed over the Yellow Sea and reached Incheon. The time they remained over the Yellow Sea was approximately 5–8 h. This means that there was sufficient time for Asian dust to be mixed or react with airborne pollutants. The low-*Z* particle EPMA measurement provided a strong indication of aging process of ADS particles during long-range transport. Figure 12 presents the aging process.

Initially, when the Asian dust storm event started, mineral dust particles in the dust source region were lifted and suspended in the air, resulting in a dramatically increased mass concentration of ambient particulate matter. These particles, which were comprised mostly of minerals, such as calcite, quartz, montmorillonite, feldspars, cristobalite, muscovite, and vermiculite (Jung, et al., 2010; Malek, et al., 2011), were transported by strong westerly winds to the middle and eastern China, where many types of air pollutants (e.g. SO<sub>2</sub>, NO<sub>2</sub>, NH<sub>3</sub>, soot, and organic matters) from power plants, motor vehicles, cooking, biomass burning, etc. were emitted (Lee et al., 2013). Industrial growth in China might increase the emission of anthropogenic pollutants due to

Title Page

Abstract

Introduction

Conclusions

References

Tables

Figures

◀

▶

◀

▶

Back

Close

Full Screen / Esc

Printer-friendly Version

Interactive Discussion



Investigation of aged,  
size-resolved Asian  
dust storm particles

H. Geng et al.

Title Page

Abstract

Introduction

Conclusions

References

Tables

Figures

◀

▶

◀

▶

Back

Close

Full Screen / Esc

Printer-friendly Version

Interactive Discussion



the increased use of fossil-fuels in factories, power-plants, and vehicles. In addition, vast anthropogenic magnetic particulates, particularly carbon-bearing iron-oxides, are produced (Kim et al., 2012). When dust particles leave the continent and enter the marine atmosphere, they normally experience significant modification by the surface uptake of gaseous species and mixing with other particulate matter. A large number of the particles might rapidly become a mixture of mineral, sea salt, sulfate, and/or nitrate in the marine atmosphere (Fan et al., 1996).

During transport, reactive gases (e.g.  $\text{SO}_2$ ,  $\text{NO}_2$ , etc.) are likely to be adsorbed on some of the dust particles and then oxidize to their acidic forms or acidic gases (e.g.  $\text{HNO}_3$  and  $\text{H}_2\text{SO}_4$ ); sometimes, their ammonium salts (e.g.  $\text{NH}_4\text{NO}_3$  and  $(\text{NH}_4)_2\text{SO}_4$ ) can be adsorbed directly on the dust particles (Manktelow et al., 2010; Formenti et al., 2011; Huang et al., 2010; Li and Shao, 2012). When the acids are formed/adsorbed on the dust particles, they can be neutralized fully or partially by the alkaline species (e.g.  $\text{CaCO}_3$ ) or by ambient  $\text{NH}_3$ . In the marine air, the presence of liquid water will result in more efficient transformation of  $\text{SO}_2$  to sulfate and  $\text{NO}_x$  to nitrate, and the enrichment of sulfate and nitrate on dust particles in the marine atmosphere becomes more effective. Previous studies showed that nitrate formation on aluminosilicates and calcium carbonate is favored compared to sulfate (Ma et al., 2012; Li et al., 2012). Especially, the formation of nitrates from  $\text{CaCO}_3$  would enhance significantly the uptake of water and water-soluble species, resulting in a positive feedback until  $\text{CaCO}_3$  completely transformed to  $\text{Ca}(\text{NO}_3)_2$  (Formenti, et al., 2011). Given that no fresh SSAs were found and the majority of reacted SSAs were  $\text{NaNO}_3$ -containing, the Cl depletion from sea-salts would be caused mostly by the uptake of  $\text{HNO}_3$  (or  $\text{NO}_x$ ) rather than that of  $\text{H}_2\text{SO}_4$  (or  $\text{SO}_2$ ). The atomic concentration ratio of Cl/N in the nitrate-containing reacted SSAs is in 0.08–0.15 (Table 6), indicative of strong Cl depletion.

Moisture over the sea is favorable not only for the reaction of mineral dust with  $\text{NO}_x$  and  $\text{SO}_2$ , but also for the formation of (C, N, O, S)-rich particles, which are likely mixtures of  $\text{NH}_4\text{NO}_3$  and  $(\text{NH}_4)_2\text{SO}_4/\text{NH}_4\text{HSO}_4$  with water-soluble organic carbon (WSOC) in the atmosphere. WSOC accounts for approximately 20–35 % in the organic

carbon fraction (Pathak et al., 2011). Because OC on stage 6 in sample S1 was abundant, a large part of the OC detected in sample S1 is thought to have contributed to the formation of (C, N, O, S)-rich particles by being dissolved in airborne water droplets or by aqueous-phase processing during transport over the sea. This type of (C, N, O, S)-rich particles were abundantly encountered in samples S2 and S3. For SSAs collected in Incheon, more than 60 % of them were internally mixed with mineral dust (Fig. 10), suggesting that the mixing of mineral dust and sea salt is rather routine. Although the mechanisms responsible for the mixing of dust particles and sea salt have not been elucidated in detail (Zhang et al., 2006), particle-to-particle collisions and in-cloud processing are likely to be major routes for the agglomerate formation (Ma, 2010; Li et al., 2012). Although NaCl-containing particles were found in Beijing, they were not encountered in Incheon. It is possible that they were mixed with sea salt particles of marine origin when the particles passed over the Yellow Sea.

## 4 Conclusions

In this study, three sets of ADS particle samples collected in Beijing, China and Incheon, Korea on 28–29 April 2005 were examined by low-Z particle EPMA. Overall 4200 individual particles, including reacted or aged ADS particles, which experienced extensive chemical modification during long-range transport, were investigated. The morphology, elemental compositions, and mixing state of the particles on stages 1–6 with 50 % cut-off diameters of 16, 8, 4, 2, 1, and 0.5  $\mu\text{m}$  were analyzed (approximately 97 % of the analyzed particles were in the size range, 0.5–16  $\mu\text{m}$ ). At stages 2–5, particles of aged or reacted mineral dust were most abundant in Beijing, followed by unreacted mineral dust, carbonaceous, and Fe-rich. After the ADS passed over the sea, many aged or reacted SSAs and the mixture of SSAs with mineral dust were encountered. For the aged mineral dust and SSAs, the nitrate-containing and both nitrate- and sulfate-containing species outnumbered those only sulfate-containing species, suggesting that ambient nitrogen oxides had a larger influence on atmospheric

## Investigation of aged, size-resolved Asian dust storm particles

H. Geng et al.

Title Page

Abstract

Introduction

Conclusions

References

Tables

Figures

◀

▶

◀

▶

Back

Close

Full Screen / Esc

Printer-friendly Version

Interactive Discussion



Investigation of aged,  
size-resolved Asian  
dust storm particles

H. Geng et al.

Title Page

Abstract

Introduction

Conclusions

References

Tables

Figures

◀

▶

◀

▶

Back

Close

Full Screen / Esc

Printer-friendly Version

Interactive Discussion



particles than  $\text{SO}_2$  in this region. During the ADS event, a number of reacted or aged Mg-containing aluminosilicates were observed in addition to partially- or totally-reacted  $\text{CaCO}_3$ . The changes in the relative number abundance and the atomic concentration ratios of  $[\text{Mg}]/[\text{Al}]$  and  $[\text{Mg}]/[\text{Si}]$  between samples S2 and S3 and sample S1 suggests that a significant evolution or aging process occurred on the mineral dust when they passed over the sea. For the particles at stage 6, the most obvious characteristics is that many NaCl-containing particles in sample S1 and many (C, N, O, S)-rich and K-containing particles in samples S2 and S3 were encountered.

In light of the single-particle characterization of chemical compositions of aerosols, the reacted (aged) SSAs, organic compounds, and secondary aerosols have significant effects on the atmosphere when the ADS originating from Mongolia arrived at Korea. This study provides some details of ADS particles that experienced extensive chemical modification during long-range transport from Beijing to Incheon.

**Acknowledgements.** This study was supported by Basic Science Research Programs through the National Research Foundation of Korea (NRF) funded by the Ministry of Education, Science, and Technology (Grant 2012R1A2A1A05026329). In addition, the authors gratefully acknowledge the support of the NSFC-NRF Scientific Cooperation Program (Grant 2012K1A2B1A03000431 and 41211140241).

## References

- Arimoto, R., Kim, Y. J., Kim, Y. P., Quinn, P. K., Bates, T. S., Anderson, T. L., Gong, S., Uno, I., Chin, M., Huebert, B. J., Clarke, A. D., Shinozuka, Y., Weber, R. J., Anderson, J. R., Guazzotti, S. A., Sullivan, R. C., Sodeman, D. A., Prather, K. A., and Sokolik, I. N.: Characterization of Asian dust during ACE-Asia, *Global Planet. Change*, 52, 23–56, 2006.
- Ault, A. P., Moffet, R. C., Baltrusaitis, J., Collins, D. B., Ruppel, M. J., Cuadra-Rodriguez, L. A., Zhao, D., Guasco, T. L., Ebben, C. J., Geiger, F. M., Bertram, T. H., Prather, K. A., and Grassian, V. H.: Size-dependent changes in sea spray aerosol composition and properties with different seawater conditions, *Environ. Sci. Technol.*, 47, 5603–5612, 2013.

Investigation of aged,  
size-resolved Asian  
dust storm particles

H. Geng et al.

Title Page

Abstract

Introduction

Conclusions

References

Tables

Figures

◀

▶

◀

▶

Back

Close

Full Screen / Esc

Printer-friendly Version

Interactive Discussion



Bauer, S. E., Mishchenko, M. I., Laci, A. A., Zhang, S., Perlwitz, J., and Metzger, S. M.: Do sulfate and nitrate coatings on mineral dust have important effects on radiative properties and climate modeling?, *J. Geophys. Res.-Atmos.*, 112, D06307, doi:10.1029/2005JD006977, 2007.

5 Choël, M., Deboudt, K., Osán, J., Flament, P., and Van Grieken, R.: Quantitative determination of low-Z elements in single atmospheric particles on boron substrates by automated scanning electron microscopy-energy-dispersive X-ray spectrometry, *Anal. Chem.*, 77, 5686–92, 2005.

10 Choël, M., Deboudt, K., and Flament, P.: Evaluation of quantitative procedures for X-ray microanalysis of environmental particles, *Microsc. Res. Techniq.*, 70, 996–1002, 2007.

Choi, J. C., Lee, M., Chun, Y., Kim, J., and Oh, S.: Chemical composition and source signature of spring aerosol in Seoul, Korea, *J. Geophys. Res.-Atmos.*, 106, D16, 18067–18074, 2001.

15 Fan, X.-B., Okada, K., Niimura, N., Kai, K., Arao, K., Shi, G.-Y., Qin, Y., and Mitsuta, Y.: Mineral particles collected in China and Japan during the same Asian dust-storm event, *Atmos. Environ.*, 30, 347–351, 1996.

Fairlie, T. D., Jacob, D. J., Dibb, J. E., Alexander, B., Avery, M. A., van Donkelaar, A., and Zhang, L.: Impact of mineral dust on nitrate, sulfate, and ozone in transpacific Asian pollution plumes, *Atmos. Chem. Phys.*, 10, 3999–4012, doi:10.5194/acp-10-3999-2010, 2010.

20 Feng, Q., Endo, K. N., and Cheng, G. D.: Dust storms in China: a case study of dust storm variation and dust characteristics, *B. Eng. Geol. Environ.*, 61, 253–261, 2002.

Flament, P., Mattioli, N., Aimoz, L., Choël, M., Deboudt, K., de Jong, J., Rimetz-Planchon, J., and Weis, D.: Iron isotopic fractionation in industrial emissions and urban aerosols, *Chemosphere*, 73, 1793–1798, 2008.

25 Formenti, P., Rajot, J. L., Desboeufs, K., Saïd, F., Grand, N., Chevallier, S., and Schmechtig, C.: Airborne observations of mineral dust over western Africa in the summer Monsoon season: spatial and vertical variability of physico-chemical and optical properties, *Atmos. Chem. Phys.*, 11, 6387–6410, doi:10.5194/acp-11-6387-2011, 2011.

30 Geng, H., Park, Y., Hwang, H., Kang, S., and Ro, C.-U.: Elevated nitrogen-containing particles observed in Asian dust aerosol samples collected at the marine boundary layer of the Bohai Sea and the Yellow Sea, *Atmos. Chem. Phys.*, 9, 6933–6947, doi:10.5194/acp-9-6933-2009, 2009a.

## Investigation of aged, size-resolved Asian dust storm particles

H. Geng et al.

Title Page

Abstract

Introduction

Conclusions

References

Tables

Figures

◀

▶

◀

▶

Back

Close

Full Screen / Esc

Printer-friendly Version

Interactive Discussion



Geng, H., Jung, H.-J., Park, Y., Hwang, H., Kim, H., Kim, Y. J., Sunwoo, Y., and Ro, C.-U.: Morphological and chemical composition characteristics of summertime atmospheric particles collected at Tokchok Island, Korea, *Atmos. Environ.*, 43, 3364–3373, 2009b.

Geng, H., Ryu, J., Jung, H. J., Chung, H., Ahn, K. H., and Ro, C.-U.: Single-particle characterization of summertime Arctic aerosols collected at Ny-Ålesund, Svalbard, *Environ. Sci. Technol.*, 44, 2348–2353, doi:10.1021/es903268j, 2010.

Geng, H., Cheng, F., and Ro, C.-U.: Single-particle characterization of atmospheric aerosols collected at Gosan, Korea, during the Asian Pacific Regional Aerosol Characterization Experiment Field Campaign using low-Z (atomic number) particle electron probe X-ray microanalysis, *J. Air. Waste. Manage.*, 61, 1183–1191, doi:10.1080/10473289.2011.604292, 2011a.

Geng, H., Ryu, J. Y., Maskey, S., Jung, H.-J., and Ro, C.-U.: Characterisation of individual aerosol particles collected during a haze episode in Incheon, Korea using the quantitative ED-EPMA technique, *Atmos. Chem. Phys.*, 11, 1327–1337, doi:10.5194/acp-11-1327-2011, 2011b.

Harris, E., Sinha, B., Foley, S., Crowley, J. N., Borrmann, S., and Hoppe, P.: Sulfur isotope fractionation during heterogeneous oxidation of SO<sub>2</sub> on mineral dust, *Atmos. Chem. Phys.*, 12, 4867–4884, doi:10.5194/acp-12-4867-2012, 2012.

Hatch, C. D. and Grassian, V. H.: 10th Anniversary Review: Applications of analytical techniques in laboratory studies of the chemical and climatic impacts of mineral dust aerosol in the Earth's atmosphere, *J. Environ. Monitor.*, 10, 919–934, 2008.

Hopkins, R. J., Desyaterik, Y., Tivanski, A. V., Zaveri, R. A., Berkowitz, C. M., Tyliczszak, T., Gilles, M. K., and Laskin, A.: Chemical speciation of sulfur in marine cloud droplets and particles: Analysis of individual particles from the marine boundary layer over the California current, *J. Geophys. Res.*, 113, D04209, doi:10.1029/2007JD008954, 2008.

Hwang, H. and Ro, C.-U.: Single-particle characterization of four aerosol samples collected in Chuncheon, Korea, during Asian dust storm events in 2002, *J. Geophys. Res.-Atmos.*, 110, D23201, doi:10.1029/2005JD006050, 2005.

Hwang, H. and Ro, C.-U.: Direct observation of nitrate and sulfate formations from mineral dust and sea-salts using low-Z particle electron probe X-ray microanalysis, *Atmos. Environ.*, 40, 3869–3880, 2006.



- Hwang, H., Kim, H., and Ro, C.-U.: Single-particle characterization of aerosol samples collected before and during an Asian dust storm in Chuncheon, Korea, *Atmos. Environ.*, 42, 8738–8746, 2008.
- Huang, K., Zhuang, G. S., Li, J. A., Wang, Q. Z., Sun, Y. L., Lin, Y. F., and Fu, J. S.: Mixing of Asian dust with pollution aerosol and the transformation of aerosol components during the dust storm over China in spring 2007, *J. Geophys. Res.-Atmos.*, 115, D00K13, doi:10.1029/2009JD013145, 2010.
- Huebert, B. J., Bates, T., Russell, P. B., Shi, G. Y., Kim, Y. J., Kawamura, K., Carmichael, G., and Nakajima, T.: An overview of ACE-Asia: strategies for quantifying the relationships between Asian aerosols and their climatic impacts, *J. Geophys. Res.-Atmos.*, 108, D23, doi:10.1029/2003JD003550, 2003.
- Iziomon, M. G., Lohmann, U., and Quinn, P. K.: Summertime pollution events in the Arctic and potential implications, *J. Geophys. Res.*, 111, D12206, doi:10.1029/2005JD006223, 2006.
- Jung, H., Kim, B., Ryu, J., Maskey, S., Kim, J., Sohn, J., and Ro, C.-U.: Source identification of particulate matter collected at underground subway stations in Seoul, Korea using quantitative single-particle analysis, *Atmos. Environ.*, 44, 2287–2293, doi:10.1016/j.atmosenv.2010.04.003, 2010a.
- Jung, H., Malek, M. A., Ryu, J., Kim, B., Song, Y., Kim, H., and Ro, C.-U.: Speciation of individual mineral particles of micrometer size by the combined use of attenuated total reflectance-Fourier transform-infrared imaging and quantitative energy-dispersive electron probe X-ray microanalysis techniques, *Anal. Chem.*, 82, 6193–6202, doi:10.1021/ac101006h, 2010b.
- Kim, W., Doh, S. J., and Yu, Y.: Asian dust storm as conveyance media of anthropogenic pollutants, *Atmos. Environ.*, 49, 41–50, 2012.
- Kojima, T., Buseck, P. R., Wilson, J. C., Reeves, J. M., and Mahoney, M. J.: Aerosol particles from tropical convective systems: cloud tops and cirrus anvils, *J. Geophys. Res.*, 109, D12201, doi:10.1029/2003JD004504, 2004.
- Krueger, B. J., Grassian, V. H., Laskin, A., and Cowin, J. P.: The transformation of solid atmospheric particles into liquid droplets through heterogeneous chemistry: laboratory insights into the processing of calcium containing mineral dust aerosol in the troposphere, *Geophys. Res. Lett.*, 30, 1148, doi:10.1029/2002GL016563, 2003.
- Lee, S., Ho, C.-H., Lee, Y. G., Choi, H.-J., and Song, C.-K.: Influence of transboundary air pollutants from China on the high-PM<sub>10</sub> episode in Seoul, Korea for the period 16–20 October 2008, *Atmos. Environ.*, 77, 430–439, 2013.

## Investigation of aged, size-resolved Asian dust storm particles

H. Geng et al.

Title Page

Abstract

Introduction

Conclusions

References

Tables

Figures

◀

▶

◀

▶

Back

Close

Full Screen / Esc

Printer-friendly Version

Interactive Discussion



Investigation of aged,  
size-resolved Asian  
dust storm particles

H. Geng et al.

Title Page

Abstract

Introduction

Conclusions

References

Tables

Figures

◀

▶

◀

▶

Back

Close

Full Screen / Esc

Printer-friendly Version

Interactive Discussion



- Li, J., Wang, Z., Zhuang, G., Luo, G., Sun, Y., and Wang, Q.: Mixing of Asian mineral dust with anthropogenic pollutants over East Asia: a model case study of a super-duststorm in March 2010, *Atmos. Chem. Phys.*, 12, 7591–7607, doi:10.5194/acp-12-7591-2012, 2012.
- Li, W. J. and Shao, L. Y.: Observation of nitrate coatings on atmospheric mineral dust particles, *Atmos. Chem. Phys.*, 9, 1863–1871, doi:10.5194/acp-9-1863-2009, 2009.
- Li, W. J. and Shao, L. Y.: Chemical modification of dust particles during different dust storm episodes, *Aerosol Air Qual. Res.*, 12, 1095–1104, doi:10.4209/aaqr.2011.11.0188, 2012.
- Liu, X., Van Espen, P., Adams, F., Cafmeyer, J., and Maenhaut, W.: Biomass burning in southern Africa: individual particle characterization of atmospheric aerosols and savanna fire samples, *J. Atmos. Chem.*, 36, 135–155, 2000.
- Liu, X., Zhu, J., Van Espen, P., Adams, F., Xiao, R., Dong, S., and Li, Yu.: Single particle characterization of spring and summer aerosols in Beijing: formation of composite sulfate of calcium and potassium, *Atmos. Environ.*, 39, 6909–6918, 2005.
- Liu, Z. Y., Fairlie, T. D., Uno, I., Huang, J. F., Wu, D., Omarb, A., Kar, J., Vaughan, M., Rogers, R., Winker, D., Treppe, C., Hu, Y. X., Sun, W. B., Lin, B., and Cheng, A. N.: Transpacific transport and evolution of the optical properties of Asian dust, *J. Quant. Spectrosc. Ra.*, 116, 24–33, 2013.
- Ma, C. J.: Chemical transformation of individual Asian Dust particles estimated by the novel double detector system of Micro-PIXE, *Asian Journal of Atmos. Environ.*, 4, 106–114, doi:10.5572/ajae.2010.4.2.106, 2010.
- Ma, C. J., Tohno, S., Kasahara, M., and Hayakawa, S.: Properties of individual Asian dust storm particles collected at Kosan, Korea during ACE-Asia, *Atmos. Environ.*, 38, 1133–1143, 2004.
- Ma, Q., Liu, Y., Liu, C., Ma, J., and He, H.: A case study of Asian dust storm particles: chemical composition, reactivity to SO<sub>2</sub> and hygroscopic properties, *J. Environ. Sci.*, 24, 62–71, 2012.
- Malek, M. A., Kim, B., Jung, H., Song, Y., and Ro, C.-U.: Single-particle mineralogy of Chinese soil particles by the combined use of low-Z particle electron probe X-ray microanalysis and attenuated total reflectance-FT-IR imaging techniques, *Anal. Chem.*, 83, 7970–7977, doi:10.1021/ac201956h, 2011.
- Manktelow, P. T., Carslaw, K. S., Mann, G. W., and Spracklen, D. V.: The impact of dust on sulfate aerosol, CN and CCN during an East Asian dust storm, *Atmos. Chem. Phys.*, 10, 365–382, doi:10.5194/acp-10-365-2010, 2010.

Investigation of aged,  
size-resolved Asian  
dust storm particles

H. Geng et al.

Title Page

Abstract

Introduction

Conclusions

References

Tables

Figures

◀

▶

◀

▶

Back

Close

Full Screen / Esc

Printer-friendly Version

Interactive Discussion



Maskey, S., Choël, M., Kang, S., Hwang, H., Kim, H., and Ro, C.-U.: The influence of collecting substrates on the single-particle characterization of real atmospheric aerosols, *Anal. Chim. Acta.*, 658, 120–127, doi:10.1016/j.aca.2009.11.006, 2010.

Maskey, S., Geng, H., Song, Y., Hwang, H., Yoon, Y., Ahn, K., and Ro, C.-U.: Single-particle characterization of summertime Antarctic aerosols collected at King George Island using quantitative energy-dispersive electron probe X-ray microanalysis and attenuated total reflection Fourier transform-infrared imaging techniques, *Environ. Sci. Technol.*, 45, 6275–6282, doi:10.1021/es200936m, 2011.

Matsumoto, J., Takahashi, K., Matsumi, Y., Yabushita, A., Shimizu, A., Matsui, I., and Sugimoto, N.: Scavenging of pollutant acid substances by Asian mineral dust particles, *Geophys. Res. Lett.*, 33, L07816, doi:10.1029/2006GL025782, 2006.

Mori, I., Nishikawa, M., Tanimura, T., and Quan, H.: Change in size distribution and chemical composition of kosa (Asian dust) aerosol during long-range transport, *Atmos. Environ.*, 37, 4253–4263, 2003.

Natsagdorj, L., Jugder, D., and Chung, Y. S.: Analysis of dust storms observed in Mongolia during 1937–1999, *Atmos. Environ.*, 37, 1401–1411, 2003.

Nie, W., Wang, T., Xue, L. K., Ding, A. J., Wang, X. F., Gao, X. M., Xu, Z., Yu, Y. C., Yuan, C., Zhou, Z. S., Gao, R., Liu, X. H., Wang, Y., Fan, S. J., Poon, S., Zhang, Q. Z., and Wang, W. X.: Asian dust storm observed at a rural mountain site in southern China: chemical evolution and heterogeneous photochemistry, *Atmos. Chem. Phys.*, 12, 11985–11995, doi:10.5194/acp-12-11985-2012, 2012.

Pathak, R. K., Wang, T., and Wu, W. S.: Nighttime enhancement of PM<sub>2.5</sub> nitrate in ammonia-poor atmospheric conditions in Beijing and Shanghai: plausible contributions of heterogeneous hydrolysis of N<sub>2</sub>O<sub>5</sub> and HNO<sub>3</sub> partitioning, *Atmos. Environ.*, 45, 1183–1191, 2011.

Rajot, J. L., Formenti, P., Alfaro, S., Desboeufs, K., Chevaillier, S., Chatenet, B., Gaudichet, A., Journet, E., Marticorena, B., Triquet, S., Maman, A., Mouget, N., and Zakou, A.: AMMA dust experiment: an overview of measurements performed during the dry season special observation period (SOP0) at the Banizoumbou (Niger) supersite, *J. Geophys. Res.*, 113, D00C14, doi:10.1029/2008jd009906, 2008.

Ro, C.-U., Osan, J., Szalowski, I., Oh, K. Y., and Van Grieken, R.: Determination of chemical species in individual aerosol particles using ultrathin window EPMA, *Environ. Sci. Technol.*, 34, 3023–3030, 2000.

## Investigation of aged, size-resolved Asian dust storm particles

H. Geng et al.

Title Page

Abstract

Introduction

Conclusions

References

Tables

Figures

◀

▶

◀

▶

Back

Close

Full Screen / Esc

Printer-friendly Version

Interactive Discussion



Ro, C.-U., Oh, K.-Y., Kim, H., Chun, Y.-S., Osan, J., de Hoog, J., and Van Grieken, R.: Chemical speciation of individual atmospheric particles using low-Z electron probe X-ray microanalysis: characterizing “Asian Dust” deposited with rainwater in Seoul, Korea, *Atmos. Environ.*, 35, 4995–5005, 2001.

5 Ro, C.-U., Osán, J., Szalóki, I., de Hoog, J., Worobiec, A., and Van Grieken, R.: A Monte Carlo program for quantitative electron-induced X-ray analysis of individual particles, *Anal. Chem.*, 75, 851–859, 2003.

Ro, C.-U., Kim, H., and Van Grieken, R.: An expert system for chemical speciation of individual particles using low-Z particle electron probe X-ray microanalysis data, *Anal. Chem.*, 76, 1322–1327, 2004.

10 Schulz, M., Prospero, J. M., Baker, A. R., Dentener, F., Ickes, L., Liss, P. S., Mahowald, N. M., Nickovic, S., García-Pando, C. P., Rodríguez, S., Sarin, M., Tegen, I., and Duce, R. A.: Atmospheric transport and deposition of mineral dust to the ocean: implications for research deeds, *Environ. Sci. Technol.*, 46, 10390–10404, 2012.

15 Shao, L. Y., Li, W. J., Xiao, Z. H., and Sun, Z. Q.: The mineralogy and possible sources of spring dust particles over Beijing, *Adv. Atmos. Sci.*, 25, 395–403, 2008.

Shen, Z. X., Cao, J. J., Arimoto, R., Zhang, R. J., Jie, D. M., Liu, S. X., and Zhu, C. S.: Chemical composition and source characterization of spring aerosol over Horqin Sand Land in northeastern China, *J. Geophys. Res.*, 112, D14315, doi:10.1029/2006JD007991, 2007.

20 Sobanska, S., Hwang, H., Choël, M., Jung, H., Eom, H., Kim, H., Barbillat, J., and Ro, C.-U.: Investigation of the chemical mixing state of individual Asian dust particles by the combined use of electron probe X-ray microanalysis and Raman microspectrometry, *Anal. Chem.*, 84, 3145–3154, doi:10.1021/ac2029584, 2012.

25 Song, Y., Ryu, J., Malek, M. A., Jung, H., and Ro, C.-U.: Chemical speciation of individual airborne particles by the combined use of quantitative Energy-Dispersive Electron Probe X-ray Microanalysis and Attenuated Total Reflection Fourier Transform-Infrared Imaging Techniques, *Anal. Chem.*, 82, 7987–7998, doi:10.1021/ac1014113, 2010.

30 Song, Y.-C., Eom, H.-J., Jung, H.-J., Malek, M. A., Kim, H. K., Geng, H., and Ro, C.-U.: Investigation of aged Asian dust particles by the combined use of quantitative ED-EPMA and ATR-FTIR imaging, *Atmos. Chem. Phys.*, 13, 3463–3480, doi:10.5194/acp-13-3463-2013, 2013.

Sudheer, A. K. and Sarin, M. M.: Carbonaceous aerosols in MABL of Bay of Bengal: influence of continental outflow, *Atmos. Environ.*, 42, 4089–4100, 2008.

- Sullivan, R. C., Guazzotti, S. A., Sodeman, D. A., and Prather, K. A.: Direct observations of the atmospheric processing of Asian mineral dust, *Atmos. Chem. Phys.*, 7, 1213–1236, doi:10.5194/acp-7-1213-2007, 2007.
- Sun, Y., Zhuang, G., Huang, K., Li, J., Wang, Q., Wang, Y., Lin, Y., Fu, J. S., Zhang, W., Tang, A., and Zhao, X.: Asian dust over northern China and its impact on the downstream aerosol chemistry in 2004, *J. Geophys. Res.-Atmos.*, 115, D00k09, doi:10.1029/2009JD012757, 2010.
- Suzuki, I., Igarashi, Y., Dokiya, Y., and Akagi, T.: Two extreme types of mixing of dust with urban aerosols observed in Kosa particles: “after” mixing and “on-the-way” mixing, *Atmos. Environ.*, 44, 858–866, 2010.
- Takahashi, H., Naoe, H., Igarashi, Y., Inomata, Y., and Sugimoto, N.: Aerosol concentrations observed at Mt. Haruna, Japan, in relation to long-range transport of Asian mineral dust aerosols, *Atmos. Environ.*, 44, 4638–4644, 2010.
- Tobo, Y., Zhang, D., Matsuki, A., and Iwasaka, Y.: Asian dust particles converted into aqueous droplets under remote marine atmospheric conditions, *Proc. Natl. Acad. Sci. USA*, 107, 17905–17910, 2010.
- Usher, C. R., Michel, A. E., and Grassian, V. H.: Reactions on mineral dust, *Chem. Rev.*, 103, 4883–4940, 2003.
- Vekemans, B., Janssens, K., Vincze, L., Adams, F., and Van Espen, P.: Analysis of X-ray spectra by iterative least squares (AXIL): new developments, *X-Ray Spectrom.*, 23, 278–285, 1994.
- Wang, G. H., Zhou, B. H., Cheng, C. L., Cao, J. J., Li, J. J., Meng, J. J., Tao, J., Zhang, R. J., and Fu, P. Q.: Impact of Gobi desert dust on aerosol chemistry of Xi’an, inland China during spring 2009: differences in composition and size distribution between the urban ground surface and the mountain atmosphere, *Atmos. Chem. Phys.*, 13, 819–835, doi:10.5194/acp-13-819-2013, 2013.
- Wang, Y., Zhuang, G. S., Sun, Y. L., and An, Z. S.: Water-soluble part of the aerosol in the dust storm season – evidence of the mixing between mineral and pollution aerosols, *Atmos. Environ.*, 39, 7020–7029, 2005.
- Xuan, J., Sokolik, I. N., Hao, J., Guo, F., Mao, H., and Yang, G.: Identification and characterization of sources of atmospheric mineral dust in East Asia, *Atmos. Environ.*, 38, 6239–6252, 2004.

## Investigation of aged, size-resolved Asian dust storm particles

H. Geng et al.

Title Page

Abstract

Introduction

Conclusions

References

Tables

Figures

◀

▶

◀

▶

Back

Close

Full Screen / Esc

Printer-friendly Version

Interactive Discussion



**Investigation of aged,  
size-resolved Asian  
dust storm particles**

H. Geng et al.

Title Page

Abstract

Introduction

Conclusions

References

Tables

Figures

◀

▶

◀

▶

Back

Close

Full Screen / Esc

Printer-friendly Version

Interactive Discussion



- Yang, G. P., Zhang, H. H., Su, L. P., and Zhou, L. M.: Biogenic emission of dimethylsulfide (DMS) from the North Yellow Sea, China and its contribution to sulfate in aerosol during summer, *Atmos. Environ.*, 43, 2196–2203, 2009.
- 5 Yuan, H., Zhuang, G., Rahn, K. A., Zhang, X., and Li, Y.: Composition and mixing of individual particles in dust and nondust conditions of north China, spring 2002, *J. Geophys. Res.*, 111, D20208, doi:10.1029/2005JD006478, 2005.
- Zhang, D. Z., Iwasaka, Y., Matsuki, A., Ueno, K., and Matsuzaki, T.: Coarse and accumulation mode particles associated with Asian dust in southwestern Japan, *Atmos. Environ.*, 40, 1205–1215, 2006.
- 10 Zhang, K., Chai, F. H., Zhang, R. J., and Xue, Z. G.: Source, route and effect of Asian sand dust on environment and the oceans, *Particuology*, 8, 319–324, 2010.

Investigation of aged,  
size-resolved Asian  
dust storm particles

H. Geng et al.

**Table 1.** Sampling locations and time.

Samples	Sampling locations	Date	Time to begin sampling (UTC)	Local time for sampling (KST)	Sampling conditions
sample S1	Beijing, China	28 Apr 2005	00:45	9:45 ~ 11:00	Just after the peak time of ADS in Beijing
sample S2	Incheon, Korea	28 Apr 2005	06:00	15:00 ~ 18:55	At the beginning of ADS in Incheon
sample S3	Incheon, Korea	29 Apr 2005	00:25	9:25 ~ 11:45	At the peak time of ADS in Incheon

Title Page

Abstract

Introduction

Conclusions

References

Tables

Figures

◀

▶

◀

▶

Back

Close

Full Screen / Esc

Printer-friendly Version

Interactive Discussion





**Investigation of aged,  
size-resolved Asian  
dust storm particles**

H. Geng et al.

**Table 2.** Mean equivalent diameters ( $\mu\text{m}$ ) of the particles analyzed at different stages.

Samples	Stage 1 ( $n = 300$ )	Stage 2 ( $n = 900$ )	Stage 3 ( $n = 900$ )	Stage 4 ( $n = 900$ )	Stage 5 ( $n = 900$ )	Stage 6 ( $n = 300$ )
S1	$15.6 \pm 7.0$	$8.2 \pm 2.5$	$4.3 \pm 1.4$	$1.7 \pm 0.7$	$1.3 \pm 0.5$	$0.4 \pm 0.2$
S2	$15.3 \pm 6.9$	$7.2 \pm 2.6$	$3.7 \pm 1.4$	$2.7 \pm 0.9$	$1.3 \pm 0.6$	$0.9 \pm 0.3$
S3	$16.0 \pm 7.3$	$7.0 \pm 2.6$	$3.5 \pm 1.3$	$2.5 \pm 1.0$	$1.4 \pm 0.7$	$1.4 \pm 0.6$
Mean	$15.6 \pm 7.0$	$7.5 \pm 2.6$	$3.8 \pm 1.4$	$2.3 \pm 1.0$	$1.3 \pm 0.6$	$0.9 \pm 0.6$

Note: Units are  $\mu\text{m}$ ;  $n$  denotes the number of analyzed particles.

Title Page

Abstract

Introduction

Conclusions

References

Tables

Figures

◀

▶

◀

▶

Back

Close

Full Screen / Esc

Printer-friendly Version

Interactive Discussion



**Table 3.** Classification of the aerosol particles based on their SEIs and X-ray spectral data.

Group	Particle types	Characteristics of SEI and X-ray spectral data
1. unreacted mineral dust	aluminosilicate	Irregular and bright, having strong Al, Si, and O peaks, often with minor elements, such as Na, Mg, S, Cl, K, Ca, and Fe
	SiO <sub>2</sub>	Irregular and bright, having strong Si and O signals in its X-ray spectrum (the atomic concentration ratio of Si and O is around 1:2)
	CaCO <sub>3</sub> , MgCO <sub>3</sub> , and CaMg(CO <sub>3</sub> ) <sub>2</sub> TiO <sub>2</sub>	Appearing irregular and bright, with strong C, O, Ca and/or Mg signals in its X-ray spectrum Appearing irregular and bright, having strong Ti and O signals in its X-ray spectrum
2. reacted (or aged) mineral dust (with sulfur and nitrogen oxides or with "secondary acids" such as H <sub>2</sub> SO <sub>4</sub> and HNO <sub>3</sub> )	aged or reacted aluminosilicate, SiO <sub>2</sub> , CaCO <sub>3</sub> , CaMg(CO <sub>3</sub> ) <sub>2</sub> , etc.	Irregular and bright on their SEIs, sometimes enclosed or mixed with dark droplet, having N and/or S peaks in X-ray spectra, indicating either nitrates, sulfates, or both are generated on their surfaces
3. fresh sea salt or NaCl-containing	(Na,Mg)Cl-containing	Cubic and bright, with predominant Na and Cl signals and minor C, O, Mg, etc.
4. reacted (or aged) NaCl-containing or sea salt (and mixtures)	Nitrate-containing	Covered or enclosed with liquid, containing NO <sub>3</sub> <sup>-</sup> and/or SO <sub>4</sub> <sup>2-</sup> in addition to Na, Cl, and Mg, sometimes with detectable Al and Si and/or Ca signals
	Sulfate-containing Both nitrate- and sulfate-containing Aged sea salt mixed with mineral dust	
5. EC	carbon-rich species, including soot aggregates, tar ball, and char or coal dust	The sum of the C and O concentration is more than 90 at.%, and the concentration of C is much larger (generally more than 3 times) than that of O, and almost no other element is present
6. OC	Liquid droplet or irregular, solid particles	Irregular and solid particles, or dark droplets, with more than 90 at.% of C, O, and sometimes N (concentration of C is not much larger than that of O)
7. (C,N,O,S)-rich particles	(NH <sub>4</sub> ) <sub>2</sub> SO <sub>4</sub> /NH <sub>4</sub> HSO <sub>4</sub> -containing particles, perhaps mixed with NH <sub>4</sub> NO <sub>3</sub>	C, N, O, and S (sometimes just C, O, and S) peaks are obvious, with a lot of water-soluble organic matters inside
8. K-containing particles	Particles containing KCl or K <sub>2</sub> SO <sub>4</sub>	Irregular and bright, with K, O, S, and/or Cl peaks in their X-ray spectra
9. Fe-rich particles	FeO <sub>x</sub> or Fe(OH) <sub>x</sub>	Usually contain more than 20 at.% of Fe, generally in the form of iron ((oxy)hydr)oxides, often with minor amounts of C, Si, and Al
10. others	Only O or Cl-containing	Irregular and bright on their SEIs

Investigation of aged,  
size-resolved Asian  
dust storm particles

H. Geng et al.

**Table 4.** Relative number abundance of unreacted and reacted  $\text{CaCO}_3/\text{CaMg}(\text{CO}_3)_2$  in samples S1–S3.

	Relative abundance (%) in sample S1					Relative abundance (%) in sample S2					Relative abundance (%) in sample S3				
	st1	st2	st3	st4	st5	st1	st2	st3	st4	st5	st1	st2	st3	st4	st5
1. $\text{CaCO}_3$ or $\text{CaMgCO}_3$	8	4	4	4	1	2	1	0	2	0	10	0	0	0	0
2. Reacted $\text{CaCO}_3$ or $\text{CaMgCO}_3$	2	3	5	2	4	11	18	17	12	6	15	12	17	7	1
Nitrate-containing	1	3	4	2	3	11	7	3	2	1	5	5	0	0	0
Sulfate-containing	0	0	1	0	0	0	1	5	0	1	8	4	9	5	1
Both-containing	1	0	0	0	1	0	10	9	1	4	2	3	8	2	0
3. Sum of (1 + 2)	10	7	9	6	5	13	19	17	14	6	25	12	17	7	1

Title Page

Abstract

Introduction

Conclusions

References

Tables

Figures

◀

▶

◀

▶

Back

Close

Full Screen / Esc

Printer-friendly Version

Interactive Discussion



**Table 5.** Relative number abundances (%) of various types of aluminosilicates in samples S1–S3.

Types based on X-ray signals/mineralogy	Sample S1					Sample S2					Sample S3				
	st1	st2	st3	st4	st5	st1	st2	st3	st4	st5	st1	st2	st3	st4	st5
<b>1. Unreacted aluminosilicates</b>	<b>13</b>	<b>9</b>	<b>10</b>	<b>12</b>	<b>14</b>	<b>4</b>	<b>4</b>	<b>2</b>	<b>4</b>	<b>3</b>	<b>20</b>	<b>6</b>	<b>8</b>	<b>5</b>	<b>2</b>
(1) Al Si O (sometimes with minor Ca, P, or Ti), likely kaolinite	1	1	0	3	0	0	0	0	1	1	2	0	1	1	2
(2) Al Si O Fe, likely almandine	1	0	0	0	0	0	0	0	0	0	1	0	0	0	0
(3) Al Si O K (sometimes with minor Ca, Ti, or Na), likely K-feldspar or illite	2	1	1	0	1	2	0	0	0	0	3	1	1	0	0
(4) Al Si O Na (sometimes with minor Cl, Ca, or Ti), likely Na-feldspar	0	1	1	1	1	1	2	0	0	1	3	1	1	2	0
(5) Al Si O Mg, likely amesite or pyrope	1	1	3	4	7	0	0	0	0	0	3	0	1	0	0
(6) Al Si O Mg/mixture (one or more of all of Na, Fe, Ca, K, Cl, P, and Ti), likely montmorillonite or Mg-vermiculite	8	4	5	4	5	1	1	1	2	1	8	3	3	1	0
<b>2. Reacted aluminosilicates</b>	<b>40</b>	<b>66</b>	<b>61</b>	<b>66</b>	<b>57</b>	<b>26</b>	<b>35</b>	<b>46</b>	<b>28</b>	<b>31</b>	<b>23</b>	<b>45</b>	<b>40</b>	<b>32</b>	<b>33</b>
(1) Nitrate-containing	38	65	61	64	56	20	33	38	25	26	21	41	29	27	19
Al Si O N (sometimes with minor P or Ca)	2	4	3	2	2	1	3	4	5	3	2	1	0	3	5
Al Si O N Fe (sometimes with minor Ti)	5	3	4	3	3	0	0	0	0	0	3	0	0	0	2
Al Si O N K (sometimes with minor Fe or Ca)	1	5	5	3	4	3	1	1	1	0	0	2	0	0	1
Al Si O N Na (sometimes with minor Cl, K, Ca, P, or Fe)	2	6	10	5	3	5	12	5	5	4	4	16	4	7	2
Al Si O N Mg (sometimes with minor Cl, Ca, or K)	7	9	6	20	21	4	1	2	6	1	3	1	0	1	4
Al Si O N Mg/mixture	21	38	33	32	23	7	16	26	9	17	9	21	25	15	5
(2) Sulfate-containing	1	0	0	0	0	1	0	1	0	0	1	0	2	0	0
Al Si O S	0	0	0	0	0	0	0	0	0	0	0	0	1	0	0
Al Si O Mg S/mixture	1	0	0	0	0	1	0	0	0	0	1	0	2	0	0
(3) Both nitrate- and sulfate-containing	1	0	0	1	1	5	2	7	3	4	1	4	9	5	14
Al Si O N S (with minor Na, Fe, Ca, K, P, or Cl but without Mg)	0	0	0	0	1	2	1	2	0	1	0	3	3	1	4
Al Si O N S Mg/mixture, likely aged montmorillonite or vermiculite	1	0	0	1	0	3	1	5	3	3	1	2	6	4	10
<b>3. Sum of (1 + 2)</b>	<b>53</b>	<b>75</b>	<b>71</b>	<b>78</b>	<b>71</b>	<b>30</b>	<b>39</b>	<b>47</b>	<b>32</b>	<b>33</b>	<b>43</b>	<b>51</b>	<b>48</b>	<b>37</b>	<b>35</b>
<b>4. Percent of nitrate-containing species in all reacted aluminosilicates</b>	<b>98</b>	<b>100</b>	<b>100</b>	<b>100</b>	<b>99</b>	<b>96</b>	<b>100</b>	<b>99</b>	<b>100</b>	<b>99</b>	<b>96</b>	<b>100</b>	<b>94</b>	<b>99</b>	<b>100</b>
<b>5. Percent of Mg-containing species in the unreacted aluminosilicates</b>	<b>69</b>	<b>63</b>	<b>83</b>	<b>68</b>	<b>83</b>	<b>25</b>	<b>33</b>	<b>81</b>	<b>54</b>	<b>37</b>	<b>55</b>	<b>56</b>	<b>61</b>	<b>27</b>	<b>0</b>
<b>6. Percent of Mg-containing species in the reacted aluminosilicates</b>	<b>75</b>	<b>73</b>	<b>64</b>	<b>81</b>	<b>77</b>	<b>58</b>	<b>52</b>	<b>73</b>	<b>62</b>	<b>69</b>	<b>61</b>	<b>53</b>	<b>81</b>	<b>64</b>	<b>57</b>
<b>7. Mean of (5 + 6)</b>	<b>72</b>	<b>68</b>	<b>74</b>	<b>75</b>	<b>80</b>	<b>42</b>	<b>43</b>	<b>77</b>	<b>58</b>	<b>53</b>	<b>58</b>	<b>55</b>	<b>71</b>	<b>46</b>	<b>29</b>

## Investigation of aged, size-resolved Asian dust storm particles

H. Geng et al.

Title Page

Abstract

Introduction

Conclusions

References

Tables

Figures

◀

▶

◀

▶

Back

Close

Full Screen / Esc

Printer-friendly Version

Interactive Discussion



Investigation of aged,  
size-resolved Asian  
dust storm particles

H. Geng et al.

**Table 6.** The concentrations of elements Na, N, S, and Cl and their ratios in the reacted SSAs at different stages in samples S2 and S3.

Sample S2										Sample S3									
Atomic concentration of elements (%)						ratio of element atomic concentration				Atomic concentration of elements (%)						ratio of element atomic concentration			
(1) Nitrate-containing																			
size	n	Na	N	S	Cl	Cl/Na	Cl/N	Cl/S	S/Na	n	Na	N	S	Cl	Cl/Na	Cl/N	Cl/S	S/Na	
st1	1	17	18	0		0	0			0									
st2	47	13	17	2		0.15	0.12			17	12	14		3	0.25	0.21			
st3	48	10	17	2		0.20	0.12			26	22	17		1	0.5	0.6			
st4	62	13	15	2		0.15	0.13			29	18	17		1	0.6	0.6			
st5	56	16	12	2		0.13	0.17			3	16	12	0		0	0			
ave		14	16	2		0.13	0.11				17	15		1	0.9	0.8			
(2) Sulfate-containing																			
st1	1	17		2	4	0.24		2	0.12										
st2	1	16		6	0	0		0	0.38	1	8		12	0	0			1.5	
st3										3	8		12	1	0.13		0.08	1.5	
st4	1	9		11	0	0		0	1.22	29	12		11	1	0.8		0.9	0.92	
st5	2	16		8	0	0		0	0.50	4	18		7	0	0		0	0.39	
ave		15		7	1	0.6		0.50	0.55		12		11	1	0.5		0.4	1.08	
(3) Both-containing																			
st1	1	19	3	11	1	0.5	0.33	0.9	0.58										
st2	9	10	11	5	2	0.20	0.18	0.40	0.50	10	11	7	7	1	0.9	0.14	0.14	0.64	
st3	19	9	9	5	1	0.11	0.11	0.20	0.56	23	15	10	5	1	0.7	0.10	0.20	0.33	
st4	8	8	10	5	0	0	0	0	0.63	39	14	10	6	1	0.7	0.10	0.17	0.43	
st5	88	14	8	4	1	0.7	0.13	0.25	0.29	22	13	15	8	0	0	0	0	0.62	
ave		12	8	6	1	0.9	0.15	0.19	0.51		13	11	7	1	0.6	0.9	0.13	0.50	

**Investigation of aged,  
size-resolved Asian  
dust storm particles**

H. Geng et al.

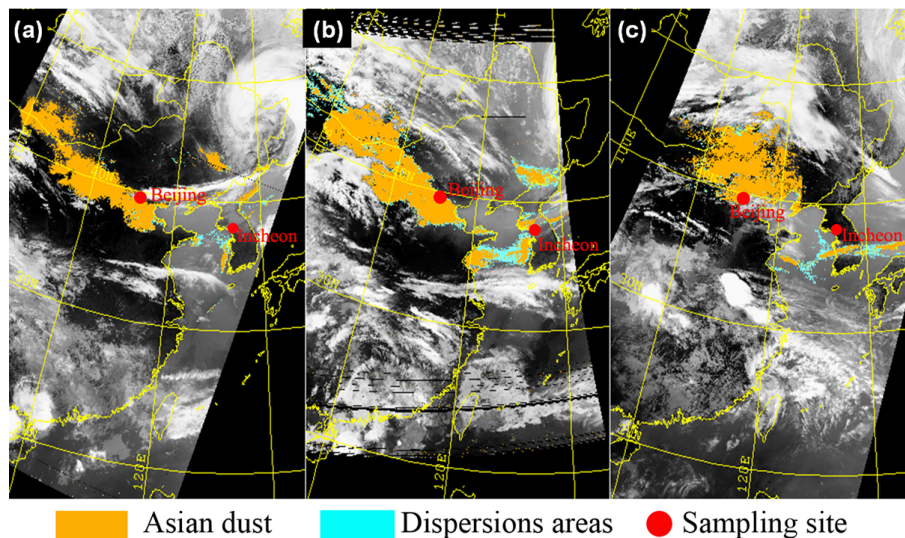


**Fig. 1.** Satellite images recorded **(a)** at 11:50 Korea Standard Time (KST) on 28 April 2005; **(b)** at 18:55 KST on 28 April 2005; and **(c)** at 11:45 KST on 29 April 2005 (provided by NOAA).

Title Page

Abstract

Introduction

Conclusions

References

Tables

Figures

◀

▶

◀

▶

Back

Close

Full Screen / Esc

Printer-friendly Version

Interactive Discussion



Investigation of aged,  
size-resolved Asian  
dust storm particles

H. Geng et al.

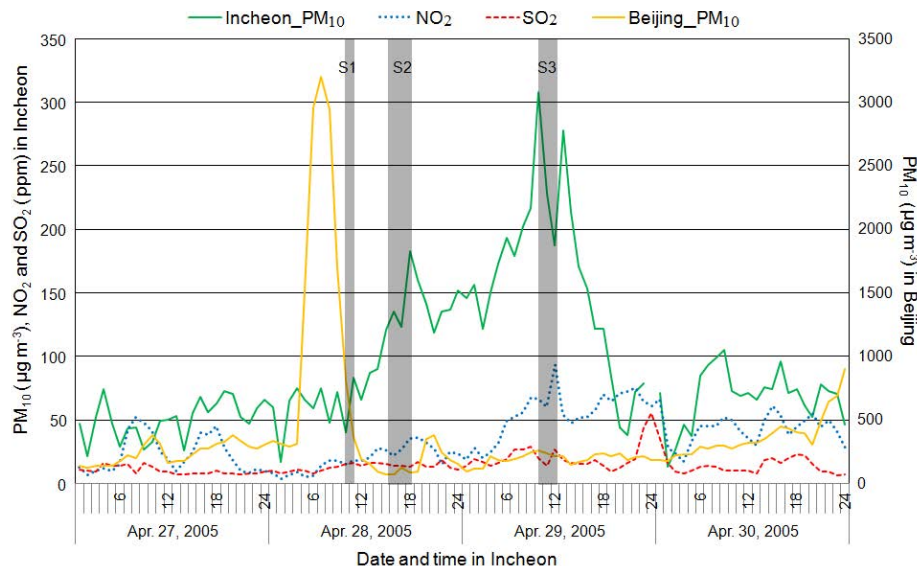


**Fig. 2.** Hourly values of PM<sub>10</sub> (in µg m<sup>-3</sup>), NO<sub>2</sub> and SO<sub>2</sub> concentrations (in ppm) recorded in Incheon (left axis) and hourly values of PM<sub>10</sub> (in µg m<sup>-3</sup>) recorded in Beijing (right axis) from 27 to 30 April 2005. The shadowed areas correspond to the sampling times of the aerosol samples S1, S2, and S3.

Title Page

Abstract

Introduction

Conclusions

References

Tables

Figures

◀

▶

◀

▶

Back

Close

Full Screen / Esc

Printer-friendly Version

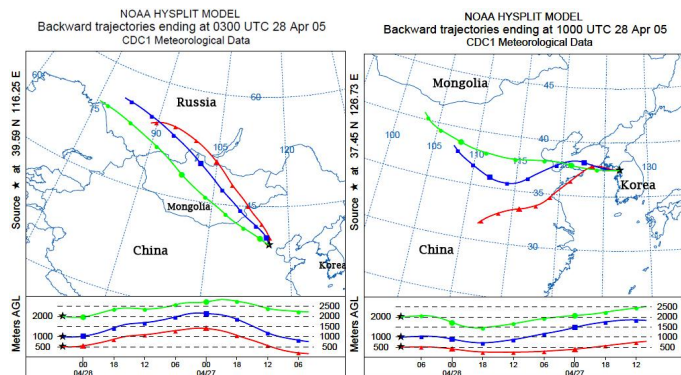
Interactive Discussion





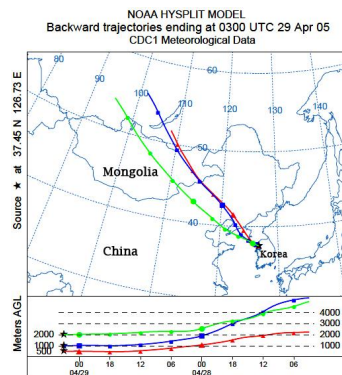
Investigation of aged,  
size-resolved Asian  
dust storm particles

H. Geng et al.



(a) At 03:00 on April 28, 2005 in Beijing

(b) At 10:00 on April 28, 2005 in Incheon



(c) At 03:00 on April 29, 2005 in Incheon

**Fig. 3.** 48 h backward trajectories of air masses ending **(a)** at 03:00 UTC on 28 April 2005 in Beijing; **(b)** at 10:00 UTC on 28 April 2005; and **(c)** at 03:00 UTC on 29 April 2005 in Incheon. Trajectory plots were produced with HYSPLIT from the NOAA ARL website: [www.arl.noaa.gov/ready/](http://www.arl.noaa.gov/ready/).

Title Page

Abstract

Introduction

Conclusions

References

Tables

Figures

◀

▶

◀

▶

Back

Close

Full Screen / Esc

Printer-friendly Version

Interactive Discussion



Investigation of aged,  
size-resolved Asian  
dust storm particles

H. Geng et al.

Title Page

Abstract

Introduction

Conclusions

References

Tables

Figures

◀

▶

◀

▶

Back

Close

Full Screen / Esc

Printer-friendly Version

Interactive Discussion

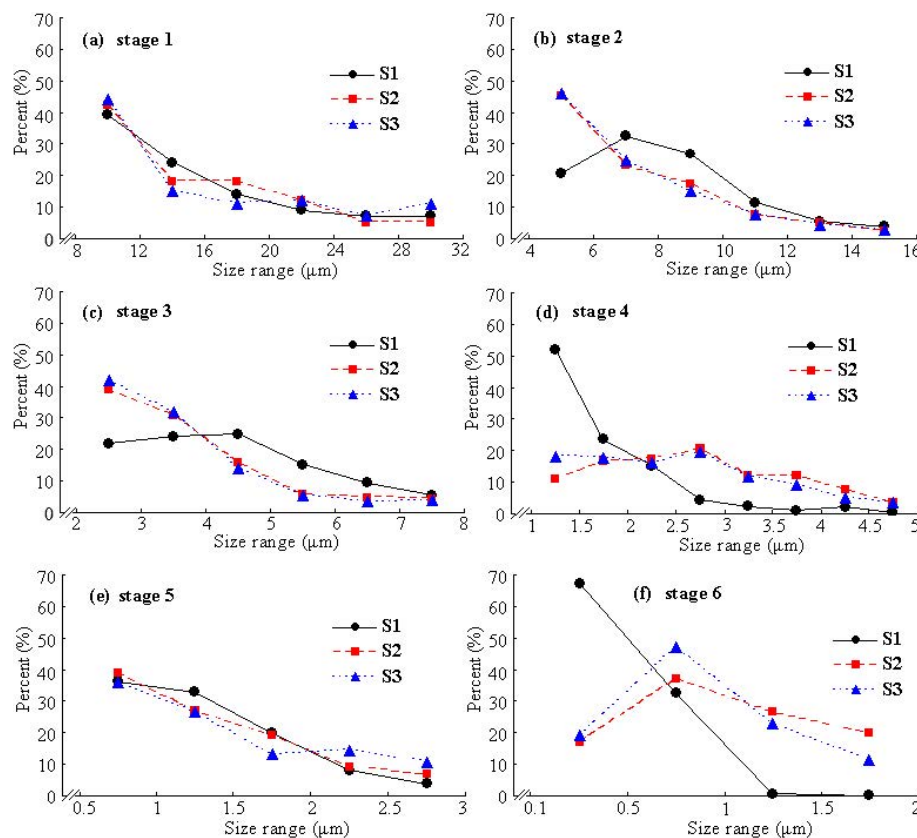
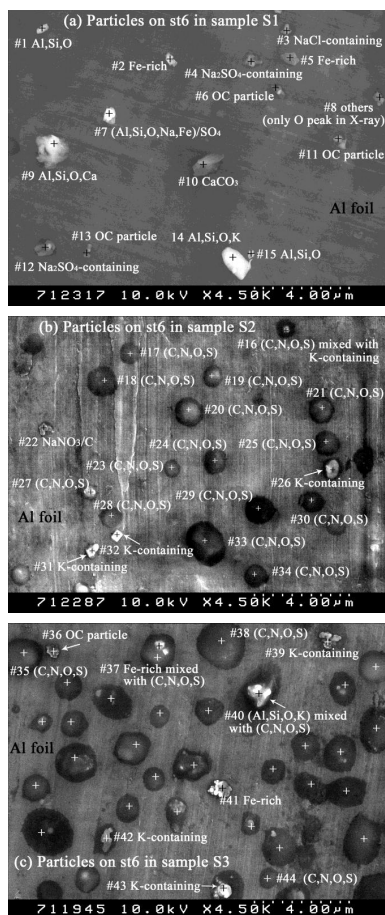


Fig. 4. Size range of analyzed particles on stages 1–6 for samples S1–S3.

Investigation of aged,  
size-resolved Asian  
dust storm particles

H. Geng et al.



**Fig. 5.** SEIs of typical particles on stage 6 in samples S1, S2, and S3. (For Fig. 5c, those with “+” are all particles rich in C, N, O, and S.)

Title Page

Abstract

Introduction

Conclusions

References

Tables

Figures

◀

▶

◀

▶

Back

Close

Full Screen / Esc

Printer-friendly Version

Interactive Discussion





Investigation of aged,  
size-resolved Asian  
dust storm particles

H. Geng et al.

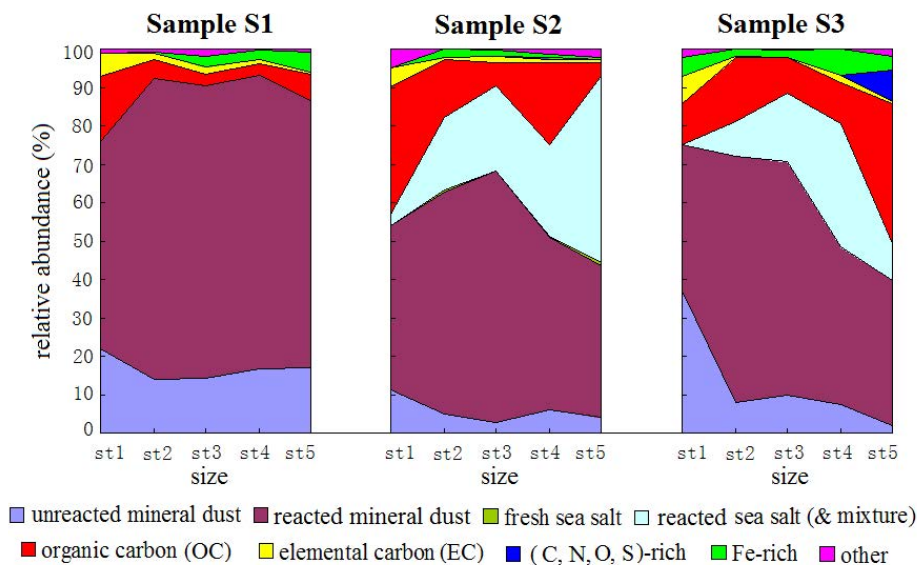


**Fig. 7.** Relative number abundances of various types of particles on stages 1–5 in samples S1–S3.

Title Page

Abstract

Introduction

Conclusions

References

Tables

Figures

◀

▶

◀

▶

Back

Close

Full Screen / Esc

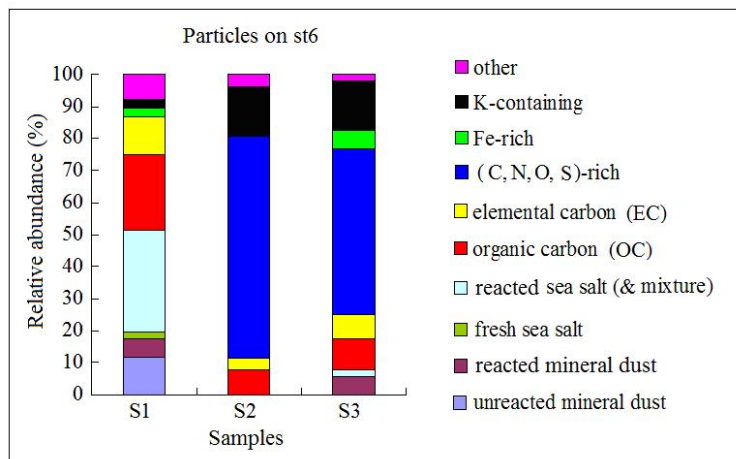
Printer-friendly Version

Interactive Discussion



**Investigation of aged,  
size-resolved Asian  
dust storm particles**

H. Geng et al.

**Fig. 8.** Relative number abundances of various types of particles on stage 6 in samples S1–S3.

Title Page

Abstract

Introduction

Conclusions

References

Tables

Figures

◀

▶

◀

▶

Back

Close

Full Screen / Esc

Printer-friendly Version

Interactive Discussion



Investigation of aged,  
size-resolved Asian  
dust storm particles

H. Geng et al.

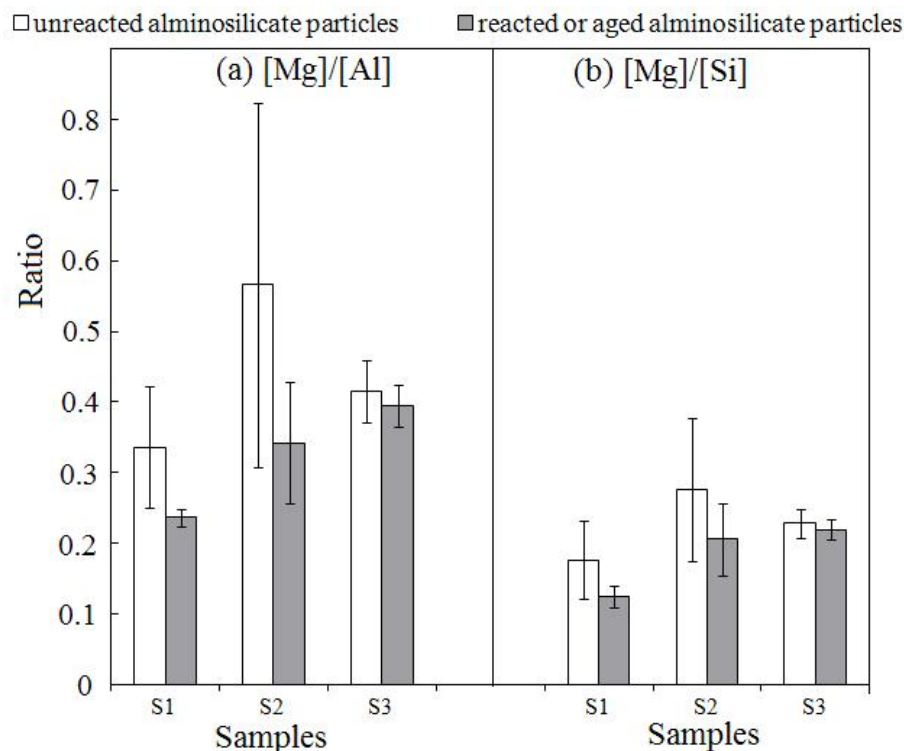


**Fig. 9.** Atomic concentration ratios of Mg/Al and Mg/Si for unreacted and reacted aluminosilicate particles in samples S1–S3 (in the unreacted aluminosilicate particles, 182 Mg-containing species were considered; and in the aged ones, 1152 were considered).

Title Page

Abstract

Introduction

Conclusions

References

Tables

Figures

◀

▶

◀

▶

Back

Close

Full Screen / Esc

Printer-friendly Version

Interactive Discussion



Investigation of aged,  
size-resolved Asian  
dust storm particles

H. Geng et al.

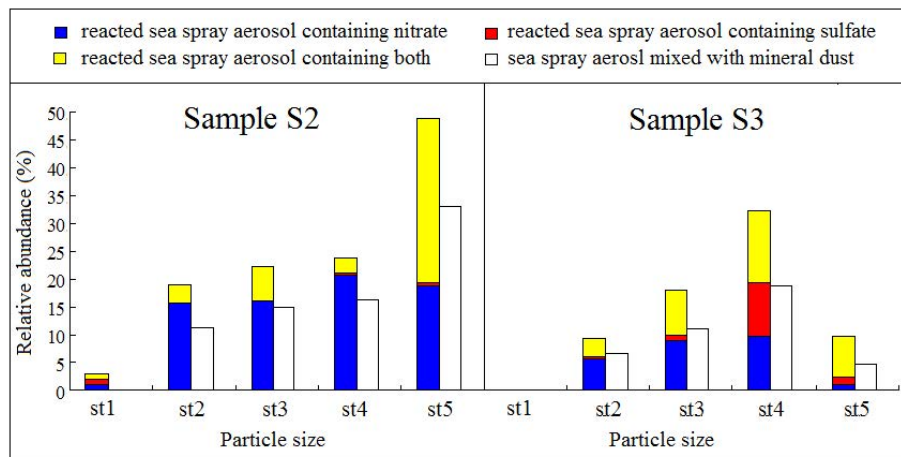


**Fig. 10.** Relative number abundances of various types of reacted sea spray aerosol (and mixture) in samples S2 and S3.

Title Page

Abstract

Introduction

Conclusions

References

Tables

Figures

◀

▶

◀

▶

Back

Close

Full Screen / Esc

Printer-friendly Version

Interactive Discussion





Investigation of aged,  
size-resolved Asian  
dust storm particles

H. Geng et al.

Title Page

Abstract

Introduction

Conclusions

References

Tables

Figures

◀

▶

◀

▶

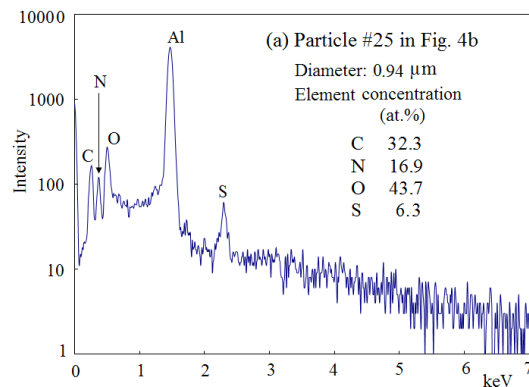
Back

Close

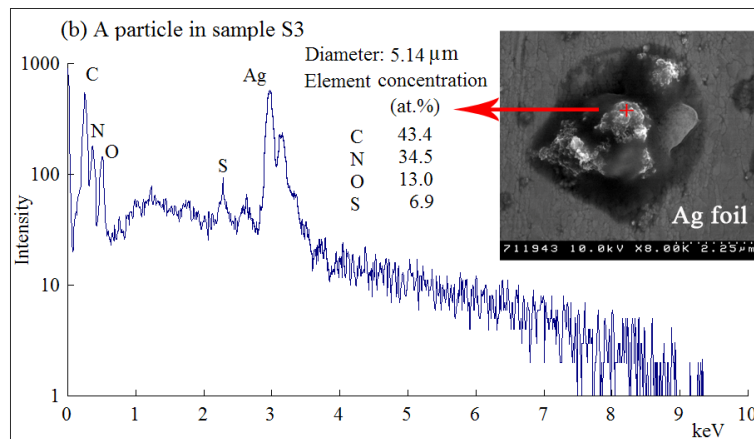
Full Screen / Esc

Printer-friendly Version

Interactive Discussion



(a) A typical particle collected on Al foil



(b) A typical particle collected on Ag foil (N concentration is relatively high)

**Fig. 11.** Typical (C, N, O, S)-rich particles. **(a)** A typical particle collected on Al foil and **(b)** a typical particle collected on Ag foil (N concentration is relatively high).

## Investigation of aged, size-resolved Asian dust storm particles

H. Geng et al.

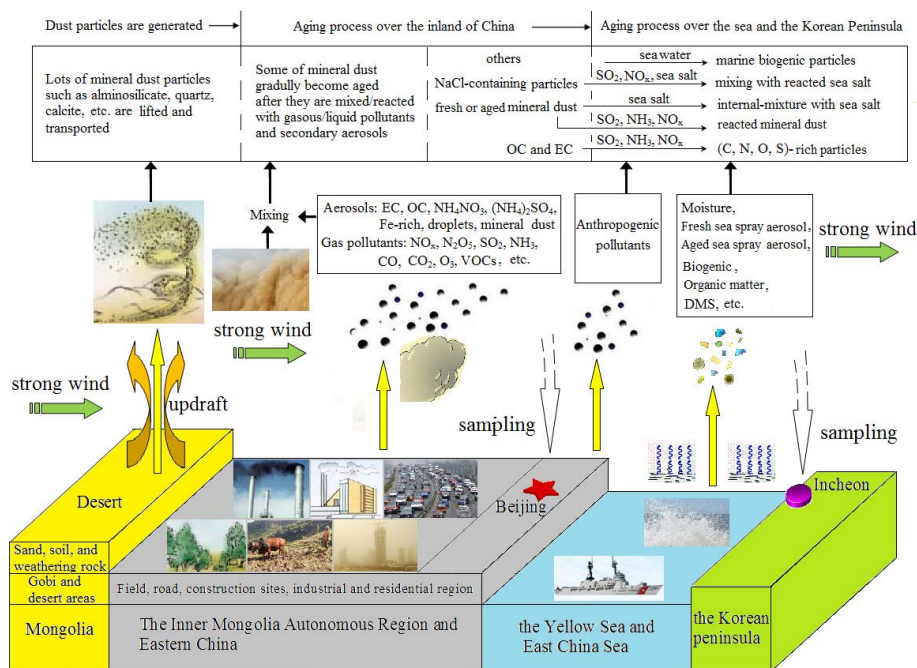


**Fig. 12.** Illustration of mixing and aging processes of Asian dust particles during long-range transport.

Title Page

Abstract

Introduction

Conclusions

References

Tables

Figures

◀

▶

◀

▶

Back

Close

Full Screen / Esc

Printer-friendly Version

Interactive Discussion